# PID and Photo Detectors Poster Session Summary


Samo Korpar
University of Maribor and J. Stefan Institute

12th Pisa Meeting on Advanced Detectors, La Biodola, May 24 – 30, 2009

In total 15 posters are presented:

- new types/variations of photo sensors - 4
- characterization and basic properties - 4
- PID methods – 3
- PID detectors and detector systems – 4

Different types of photo sensors presented: gas, vacuum, solid state and hybrid.

# New bi-dimensional SPAD arrays for Time Resolved Single Photon Imaging

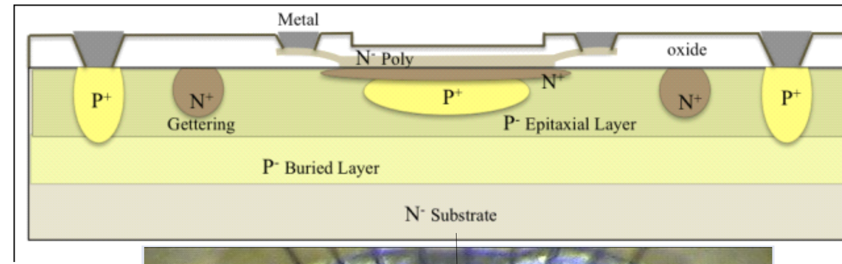


- SiPM with 2D readout of individual micro cells (SPADS)
- two quenching resistors per micro cell to connect to column and row readout
- common anodes

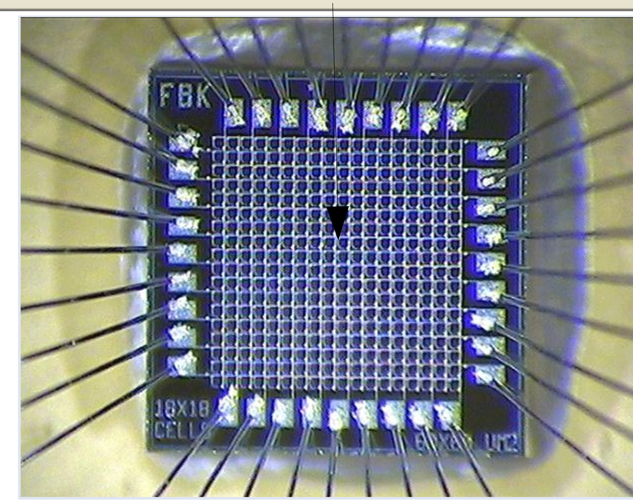


**Timing resolution**

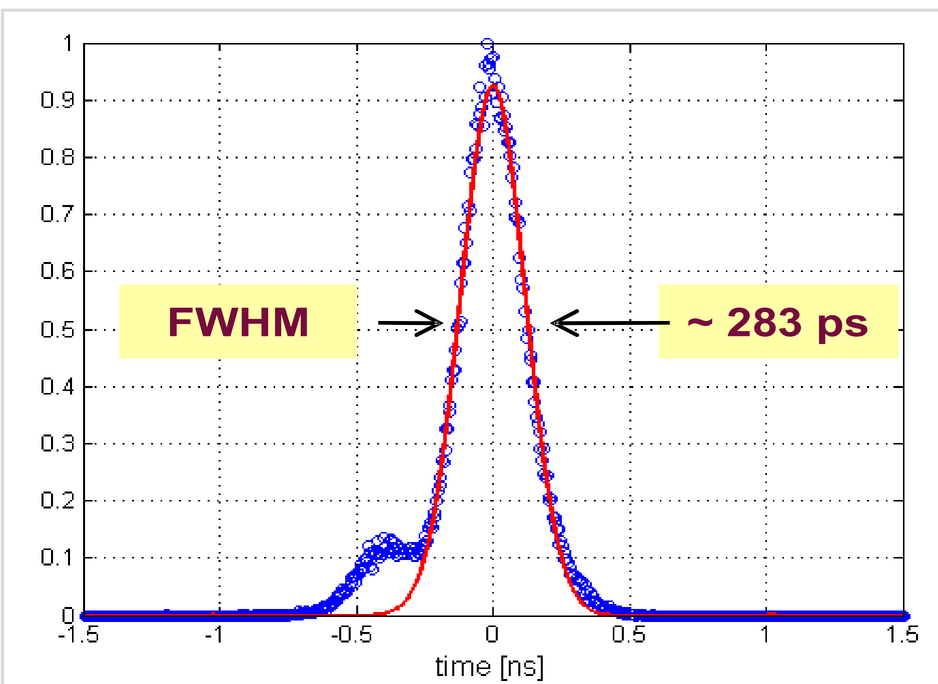


**Gain and avalanche charge Vs. bias reverse voltage**

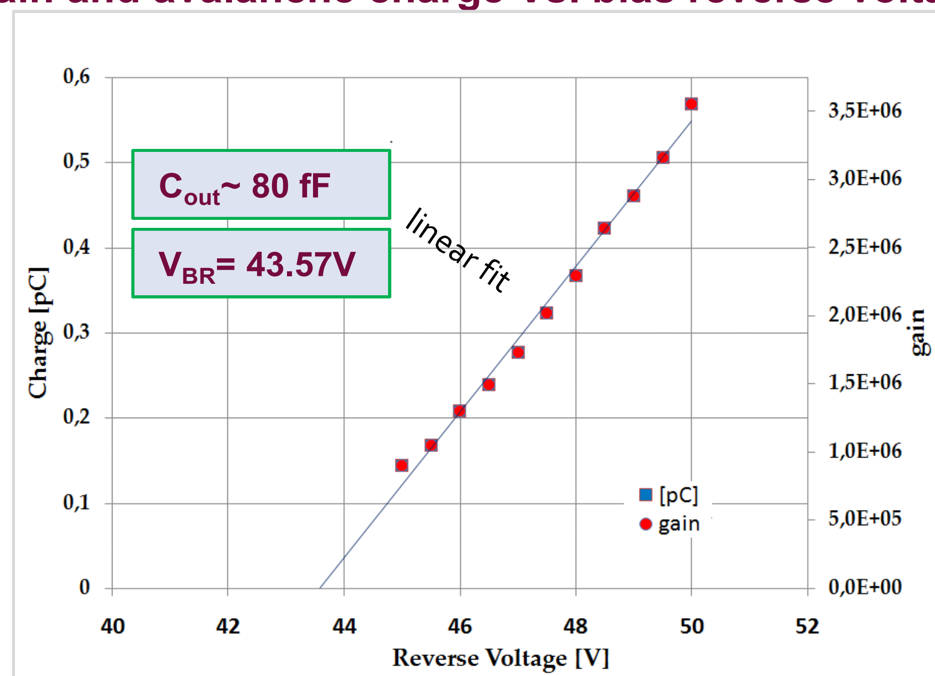


**Rosaria Grasso et al.**

# Vacuum Silicon PhotoMultipliers

- concept of hybrid photo sensor with SiPM is presented
- simulation results of photoelectron interaction with a SiPM
- preparation for electron optics study

## A new concept of detector

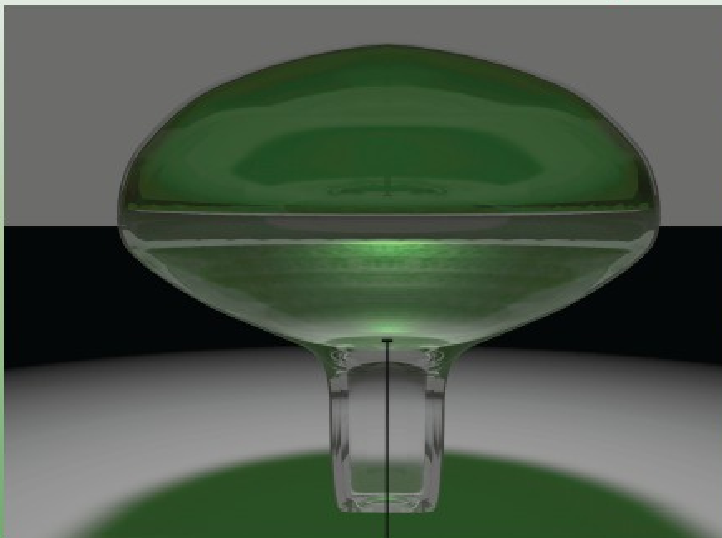

- Photocathode
- Electrostatic focusing
- SiPM as amplificator

### Advantages

- photon-counting capability
- lower operation voltages
- lower TTS

## Experimental setup

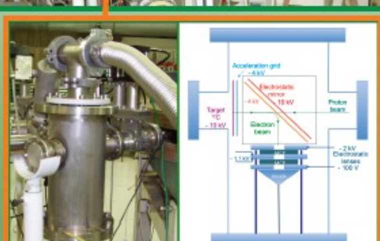

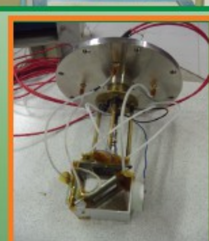

- Proton beam generated by TTT-3 Accelerator
- Electron beam obtained by stripping over $^{12}C$ target
- Electrostatic mirror
- Electrostatic lenses to focus $e^-$ beam on MCPs
- SiPM test

## Simulations

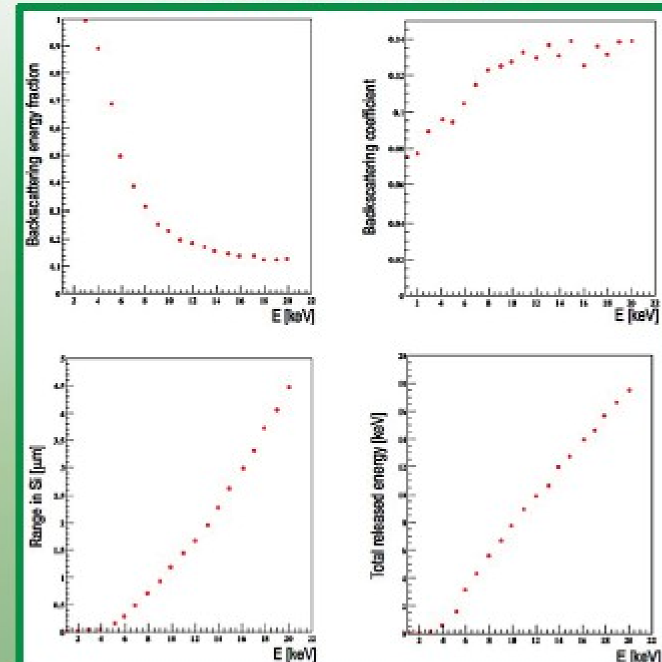


- Geant4-based simulations
- SiPM cell structure:
  - Si substrate (5mm)
  - Quartz layer (0.15 µm)
- Normally incident beam

Daniele Vivolo et al.

# Progress on the development of a silicon - carbon nanotube photodetector

**Abstract**: The properties of Carbon Nanotubes (CNTs), the new allotropic status of carbon discovered in 1991, have been widely investigated in all possible application field. This new material in fact can be easily obtained chemically by CVD (Chemical Vapour Deposition) as a layer of nanotubes growth on a wide variety of materials. When growth on a silicon surface, CNTs create a semiconductor heterojunction with peculiar photoresponsivity properties. We studied this heterojunction with the purpose to realize a large photocathode with high quantum efficiency in a large wavelength range from UV to IR. Results obtained up to day allowed us to build a new kind of photodetector very cheap, stable and easy to manage. Recently this new device has been proposed as one of candidates for the beam monitor system of SuperB.

## Silicon-CNT radiation detector

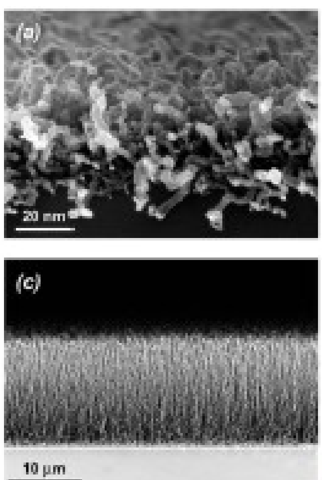


SEM image of CN device grown at a CVD temperature of 500 °C (a) and 700°C (b)


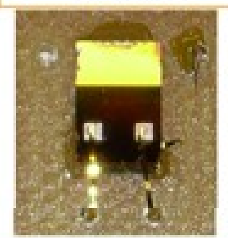

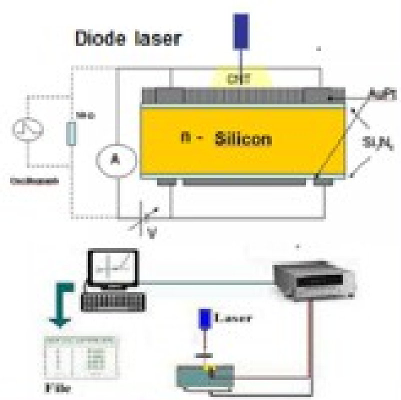


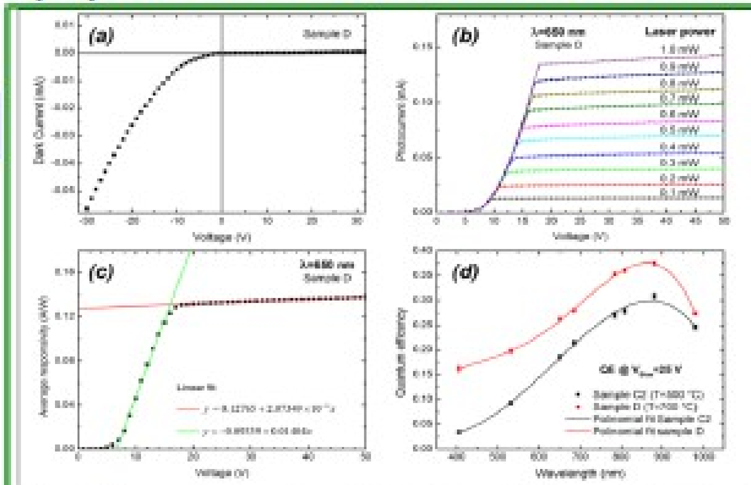


Figure 3 | Measurements performed on sample D. a, Dark current. b, I-V curve at λ=650 nm for various laser light intensities. c, Averaged responsivity at λ=650 nm. In the curves are superimposed fitting the signal rise and the current plateau. d, quantum efficiency as a function of the wavelength ranging from 405 to 980 nm of detector C2 compared with that of detector D fitted with a four order polynomial function.

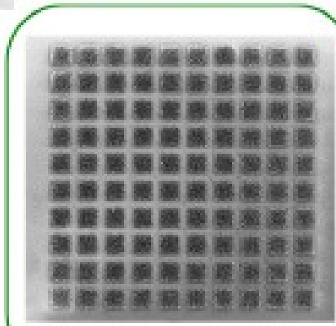

Figure 6 | 100 pixels of 4x4 µm each obtained with micro lithography.

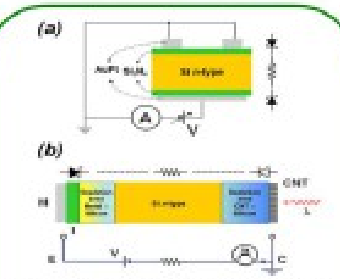


Figure 5 | Layout of CN-Si with the junctions. a, In absence of CNs the device can be schematized as a double Schottky junction polarized back-to-back. b, The presence of the CNs overbalances the system: a heterojunction is created between the CN layer and the silicon.

The presence of the CNs overbalances the system: a heterojunction is created between the CN layer and the silicon. The device shows the characteristics of a p-n-p photo-transistor, where the metallic contact on the back acts as the emitter, the upper CN layer is the collector and the CN-silicon depletion area plays the role of the transistor base. The performance of this detector depends on the CN morphology and ultimately on their electronic properties. We have found that MWCNT-based devices show a higher junction thresholds and a higher sensitivity to the UV radiation (Fig.3).

Carla Aramo et al.

# Progress on THGEM-based photon detectors for COMPASS RICH-1

- development of THGEM based photo detector for COMPASS RICH-1 upgrade
- almost all principle aspects have been validated and understood using small size prototypes
- optimization still to be performed on many detailsand open points

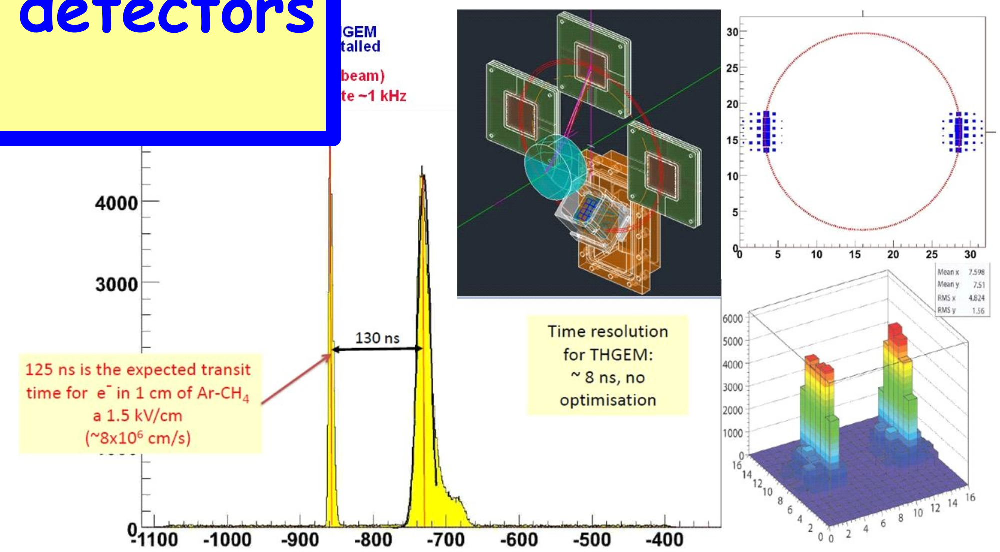


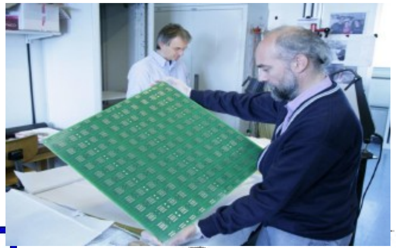

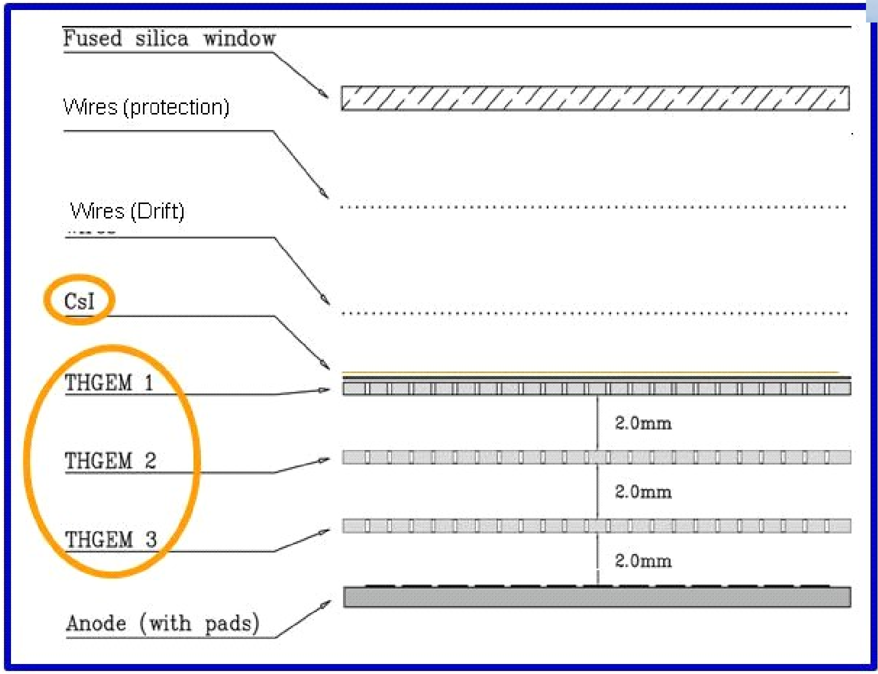


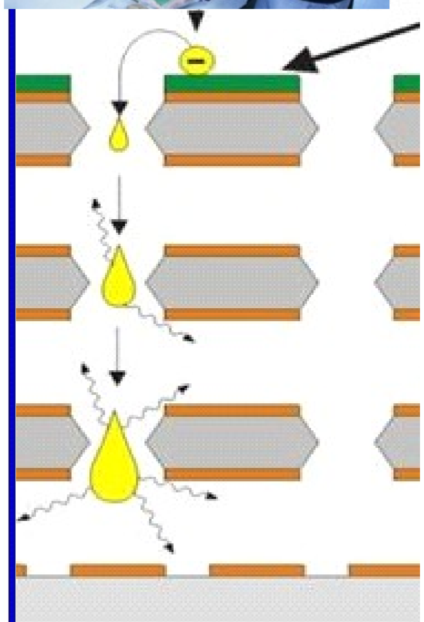

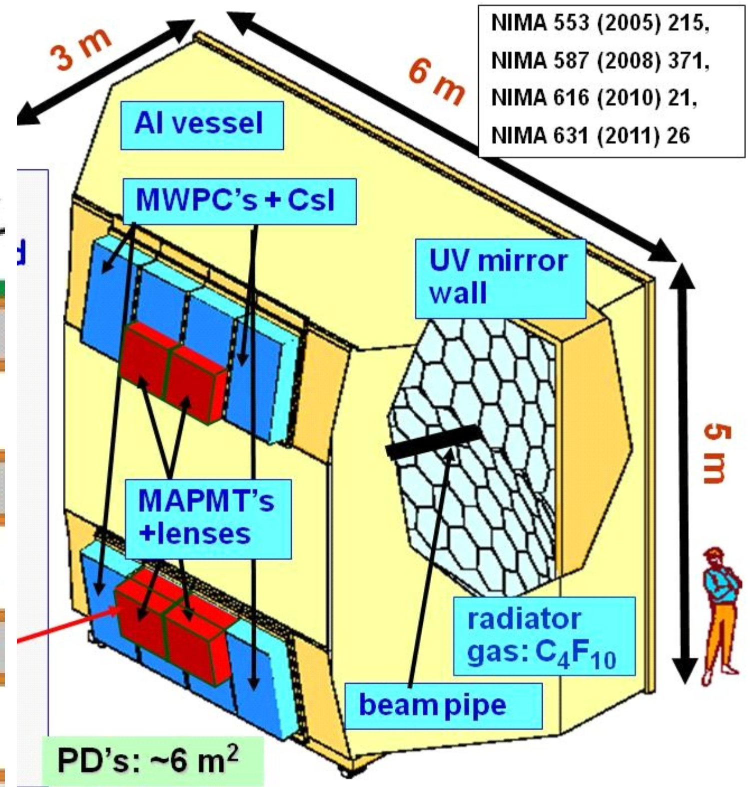


**Fulvio Tessarotto et al.**

# Ion back-flow reduction with "Flower THGEMs"

current flow for the standard triple THGEM configuration:

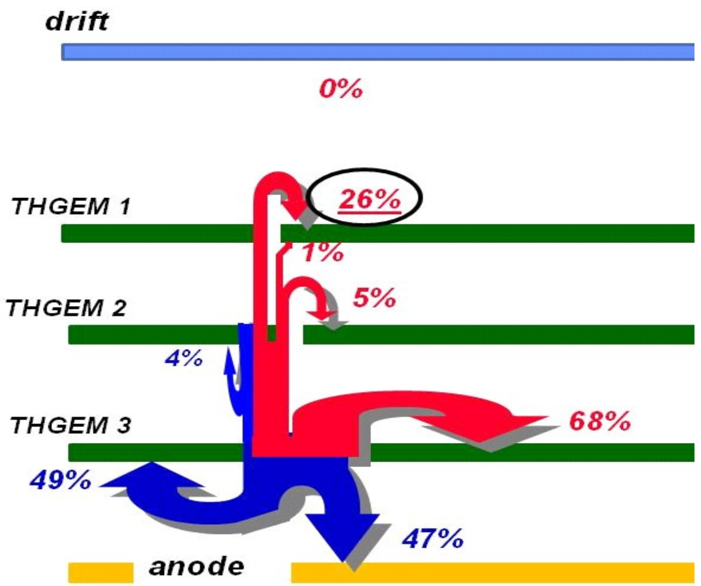


"Flower THGEM" configuration:
THGEM 1 has holes of 0.6 mm diameter, 1.2 mm pitch
THGEM 2 has holes of 0.3 mm diameter, 0.6 mm pitch, with 1/3 of the holes missing: the ones below the THGEM 1 holes

**This configuration provides charge splitting and allows for ion backflow minimization**

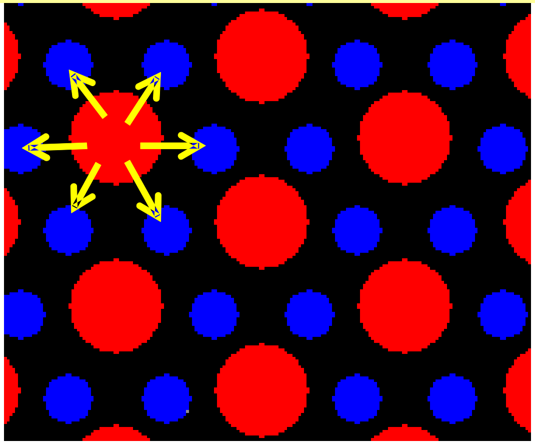

current on TOP of THGEM 1 in % for the "FLOWER" configuration:

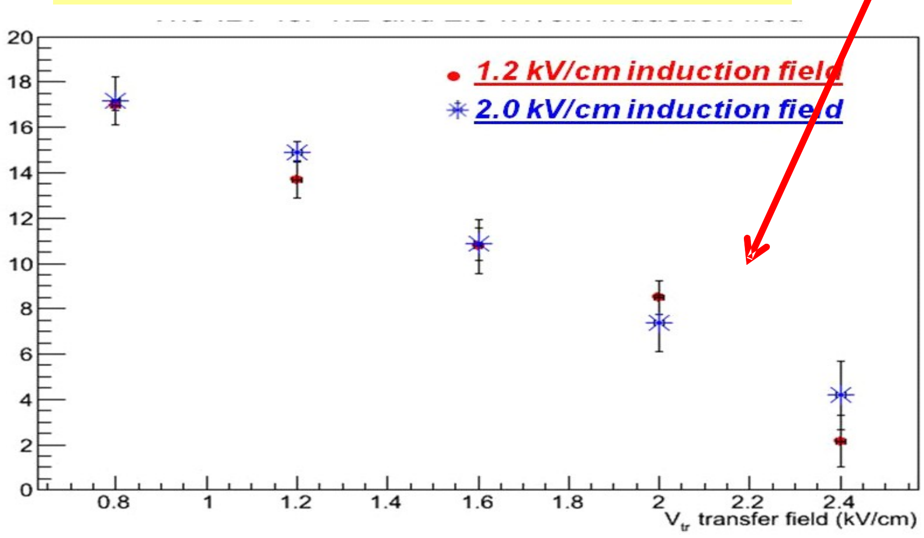


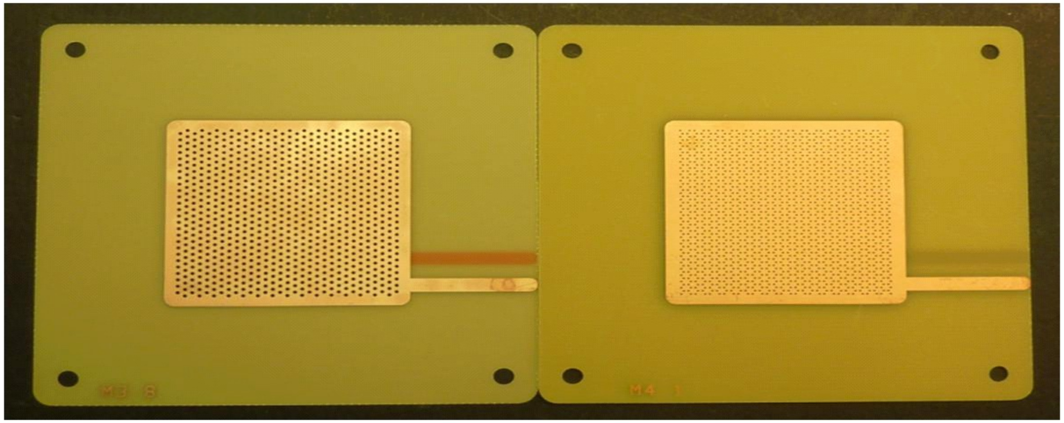

*M3.9: T=0.4mm,R=0.6mm,P=1.2mm*
*M4.1: T=0.8mm,R=0.3mm,P=0.6mm*

*Drift dis. 10.6mm*
*Transfer dis. 2.5mm*
*Induction dis. 2.5mm*

**Fulvio Tessarotto et al.**

# Photodetector time resolution: from single photons to saturation

- studies on different types of 3x3mm$^2$ SiPMs (Hamamatsu MPPC S10931-025P, S10931-050P and S10931-100P)
- readout by NINO board with TOT and LeCroy Oscilloscope DDA 735Zi 40Gs/s
- single photon time resolution σ~80 ps

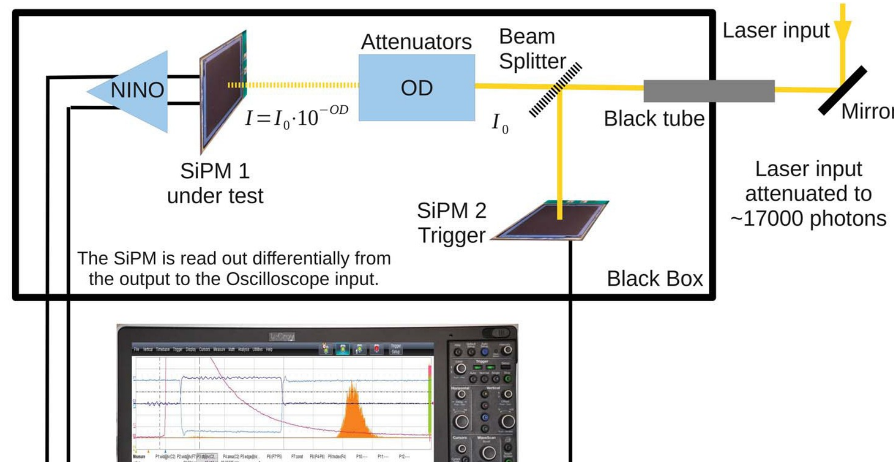


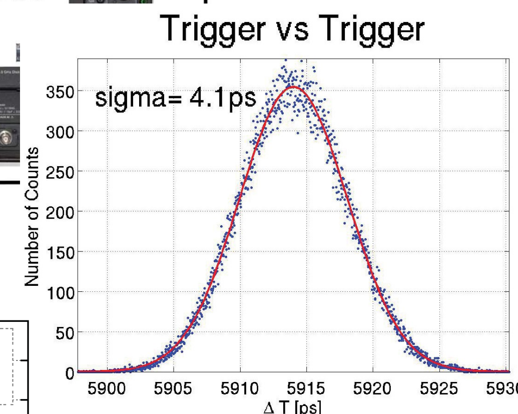


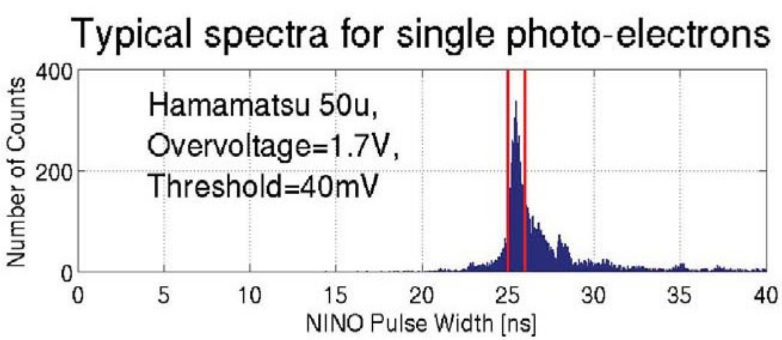


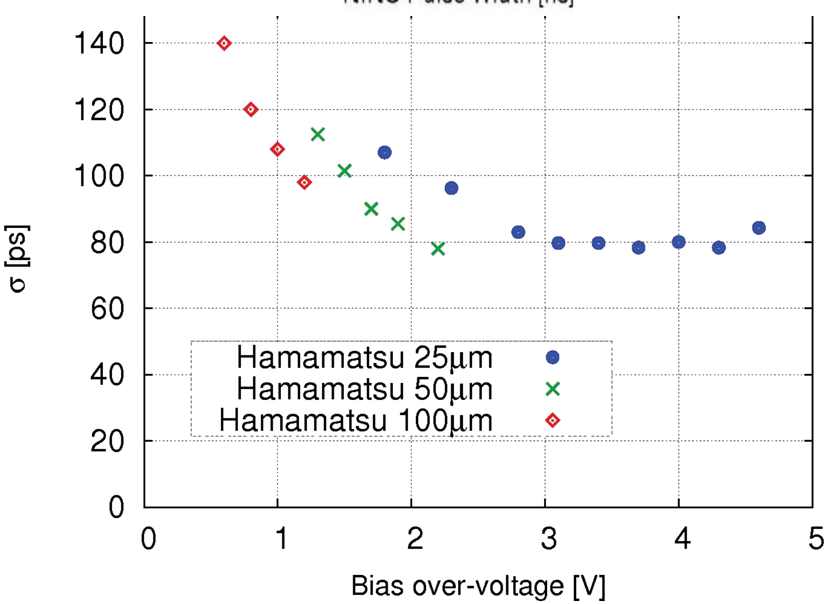


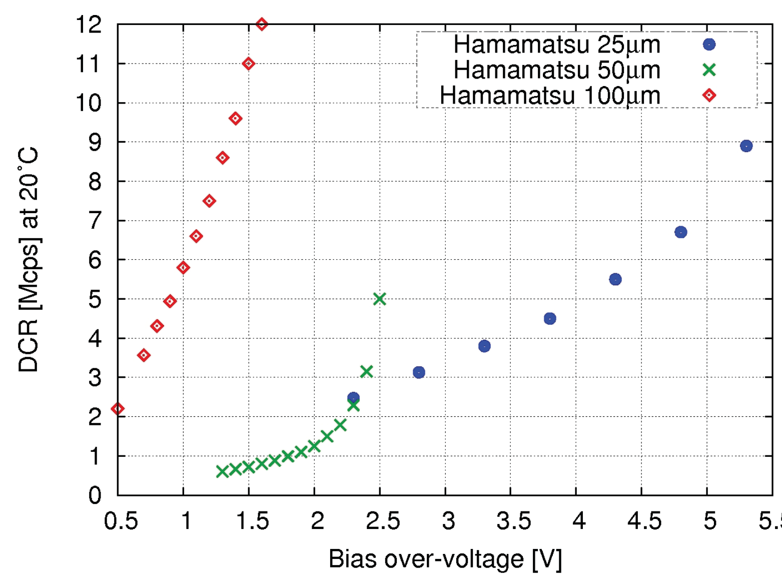


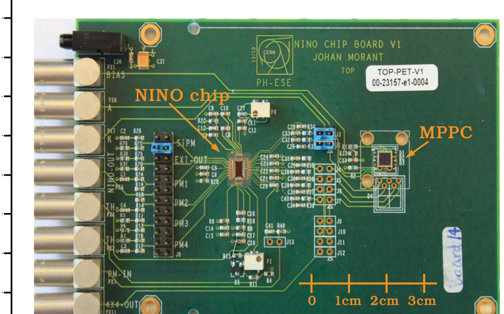


**Stefan Gundacker et al.**

# Study of H-8500 MaPMT for the FDIRC detector at SuperB

An overview of studies on the Hamamatsu H-8500 Multi-Anode Photomultiplier (MaPMT) is presented. The device will be used for the FDIRC Particle Identification detector of the SuperB experiment

**Transit Time (TT) distribution**

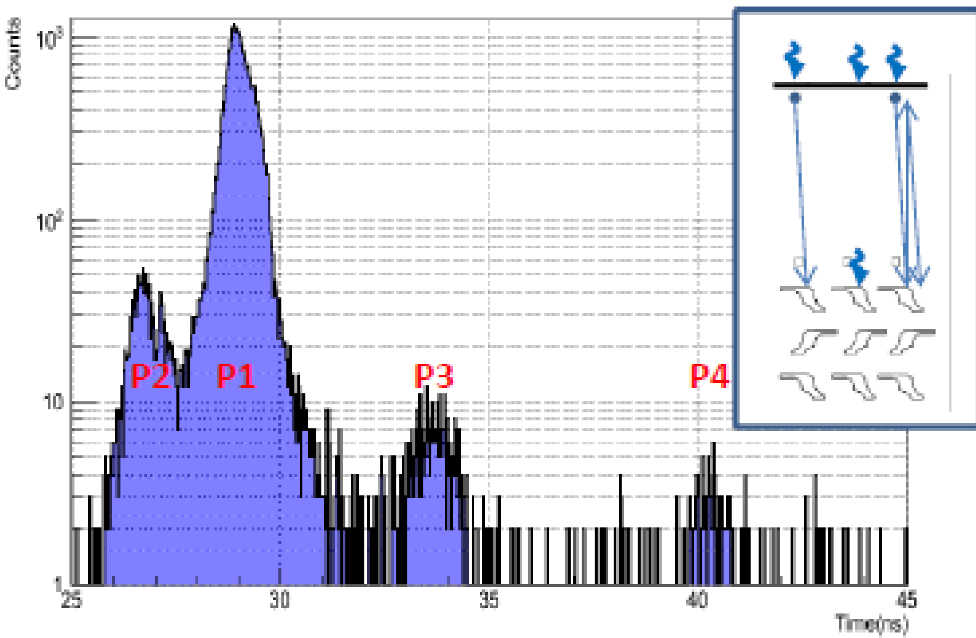


Source: focused laser beam @ 405nm

**P1**: Photons convert at photocathode and p.e. are multiplied across all the 12 dynodes.
**P2**: Photons convert at the 1st dynode and p.e. are multiplied across 11 dynodes. These p.e. are characterized by a shorter TT (-2.4ns) and a lower gain.
**P3** and **P4**: Photons convert at the photocathode but the p.e. is back scattered at the 1st dynode and then it moves again towards the 1st dynode. These p.e. are characterized by a longer TT (+4.6ns and +11.6ns).

The measured Transit Time Spread depends on the laser beam position on the photocathode and its mean value is measured to be **160-200ps.**

**Fabio Gargano et al.**

# Gain and efficiency

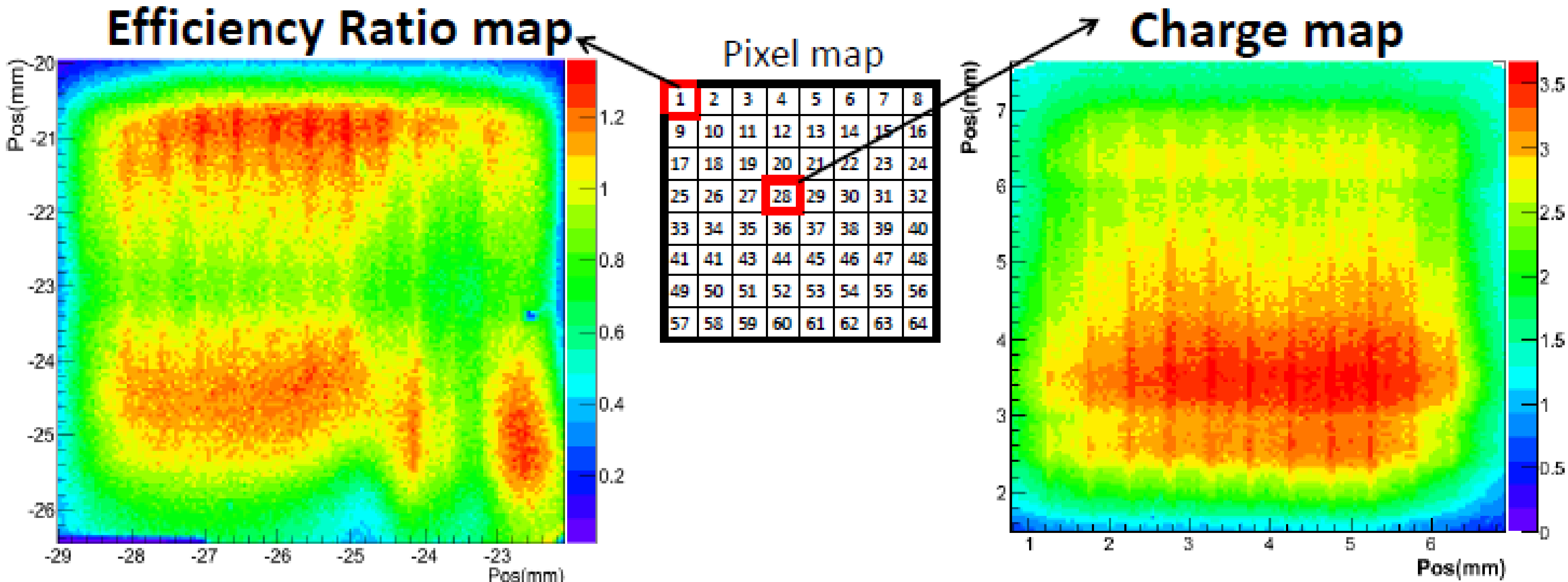


Light level @ 1 p.e.

Light level @ 20 p.e.

The map shows the ratio between H-8500 and Photonis XP2020 (reference) detection efficiency: the variation inside the pixel is roughly 50%. The increase in efficiency is also evident near the focusing electrodes.

The measured gain variation is around 50%.
The vertical lines in the map correspond to a gain increase of 5% around the focusing electrodes.

Fabio Gargano et al.

# Operation of proportional counters under high gas gain, high working gas pressure in mixed field of radiation

- gain variation in proportional counters with different gas pressure and different radiation source
- gas gain reduction at high rates/currents
- critical gas gain for nonlinear response (with $^{55}$Fe)
- $^{55}$Fe/$^{90}$Sr gas gain difference

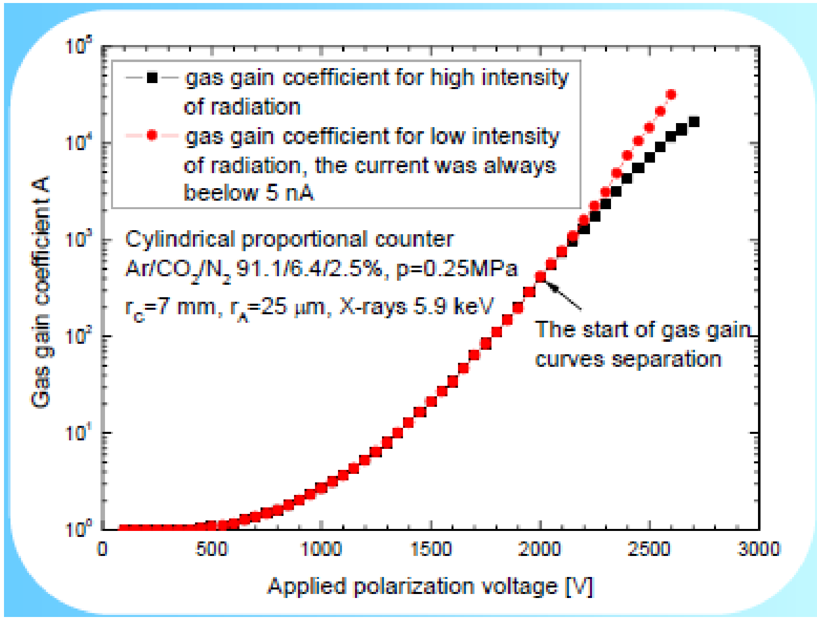


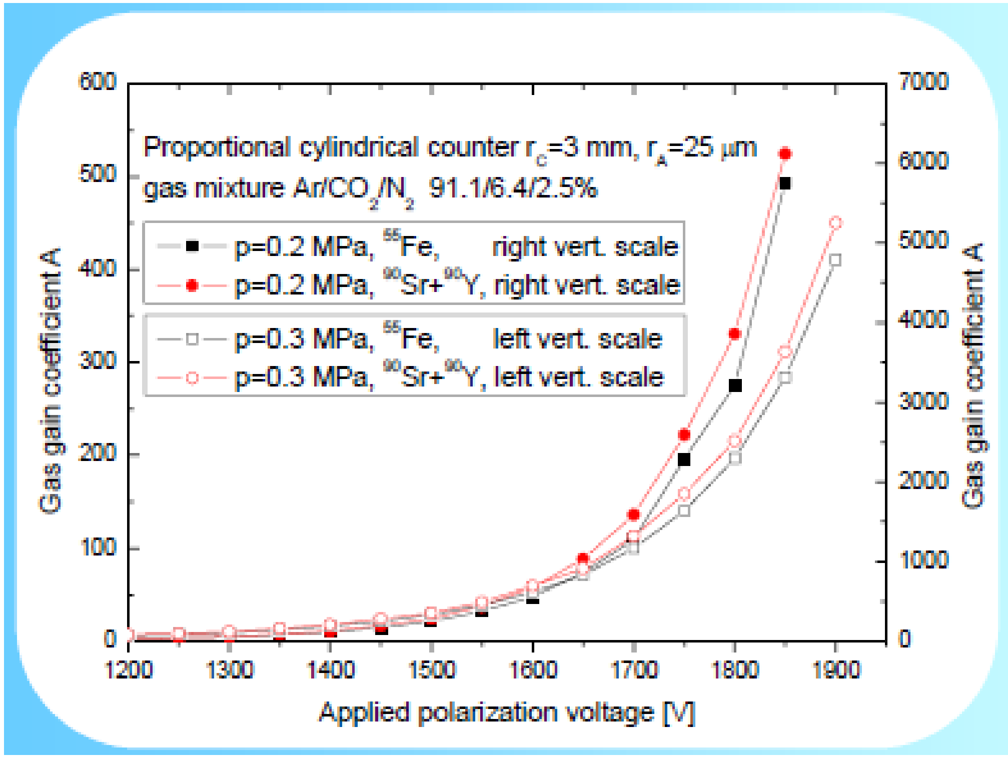


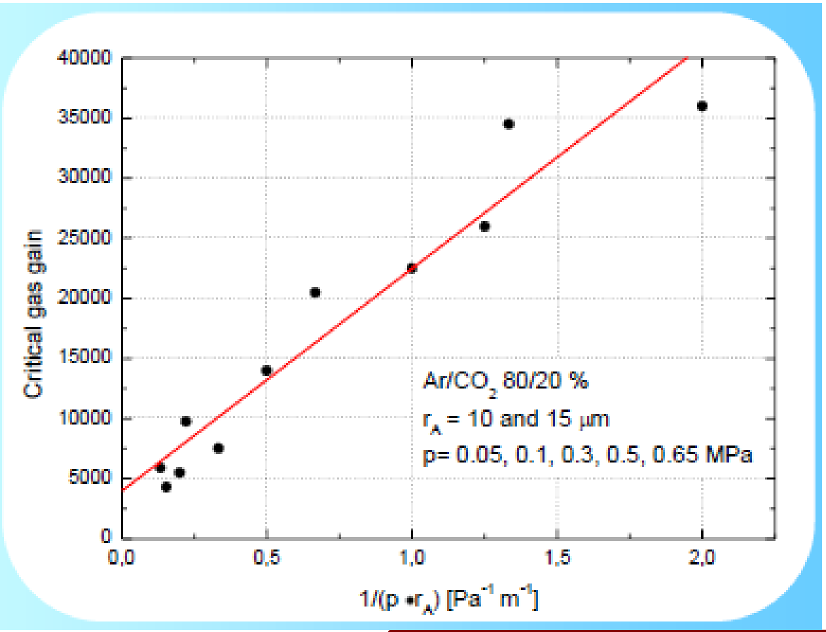


**Stefan Koperny et al.**

# EIGER characterization results

- characterisation os EIGER - next generation single photon counting x-ray detector
- x-ray camera with 22 kHz frame rat (4bit) and threshold <3keV
- 8x4cm$^2$, 0.5 Mpixel module - pixel 75μm
- 23x23cm$^2$, 9 Mpixel detector is being developed

## Characterization results

| | |
|---|---|
| Minimum noise (very low noise mode) | <100 e- |
| Threshold dispersion | <30e- (trimmed) |
| Rate capability (high speed mode) | τ < 130 ns |
| Minimum threshold (very low noise mode) | <3 keV |
| Measured frame rate (4 bit mode) | Up to 22 kHz |

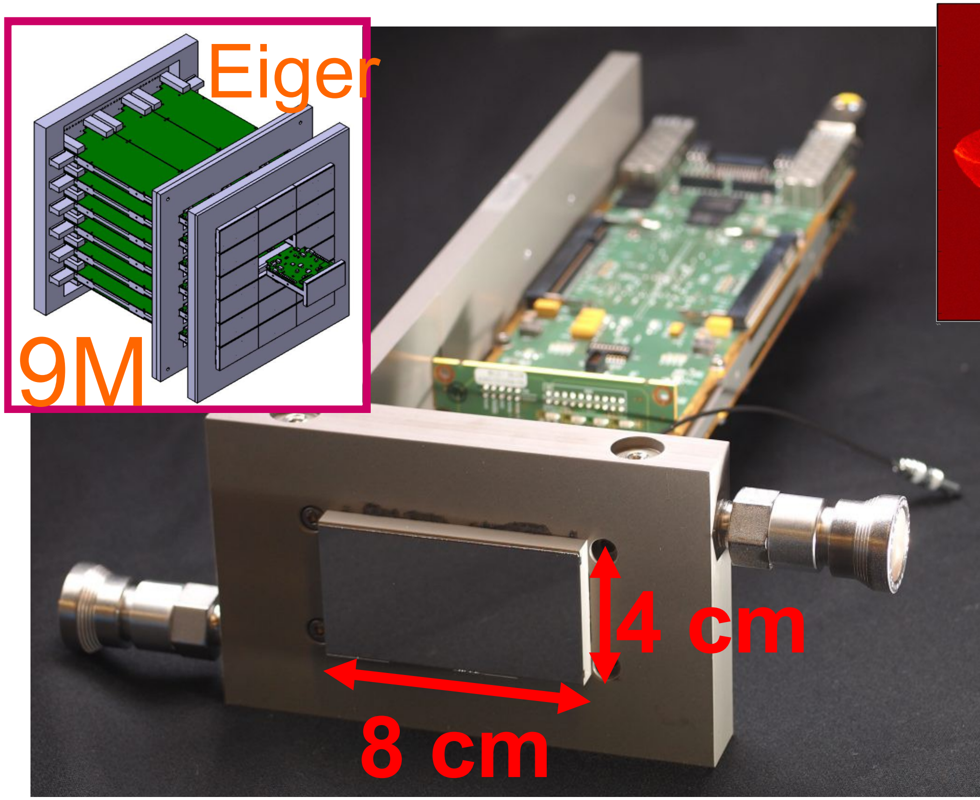


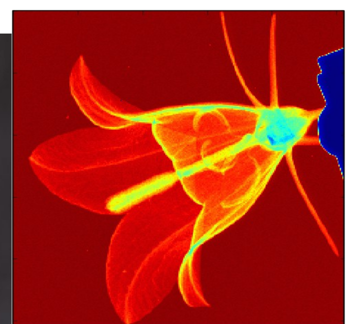

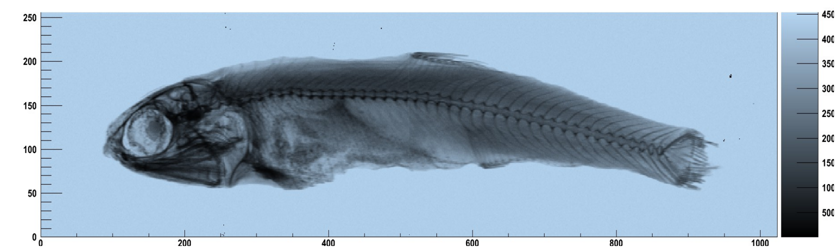

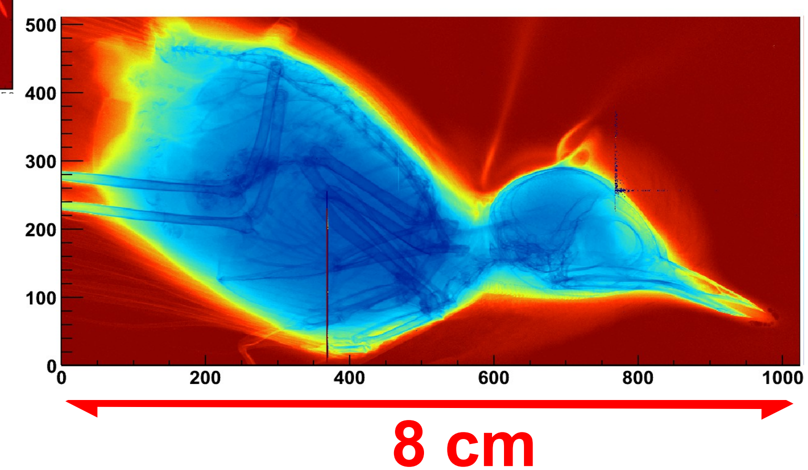


Roberto Dinapoli et al.

# Particle identification using the time-over-threshold measurements in straw tube detectors

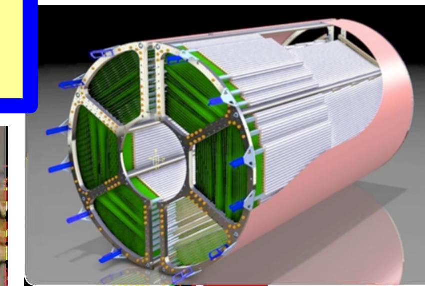

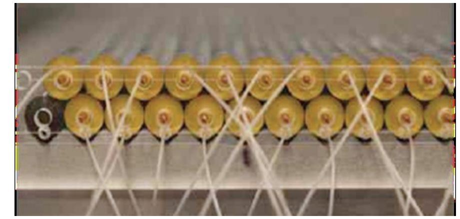

- dE/dx with PANDA Straw Tube Tracker for separation of protons, pions and kaons in the momentum range below 1 GeV/c
- verification of detector response simulation (TOT vs. charge)
- track to wire distance correction
- comparable results from TOT and charge measurement

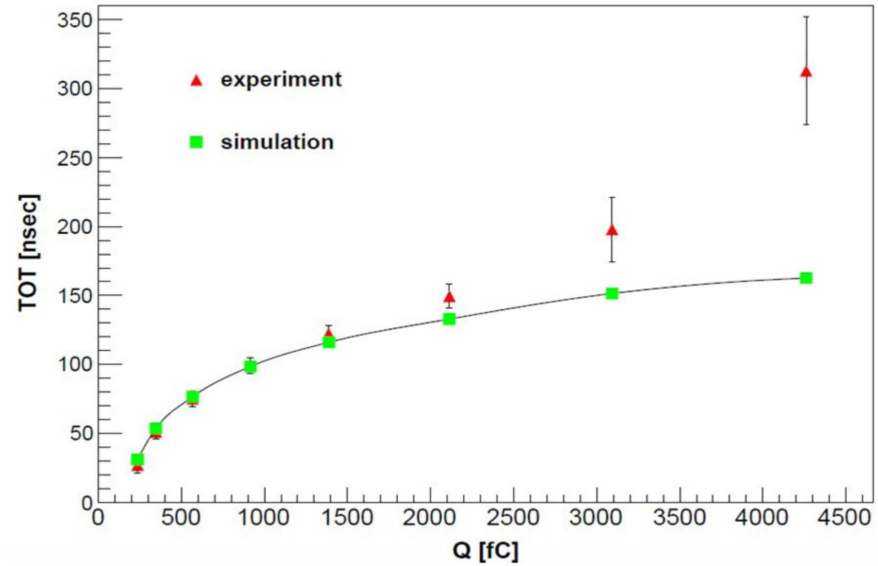


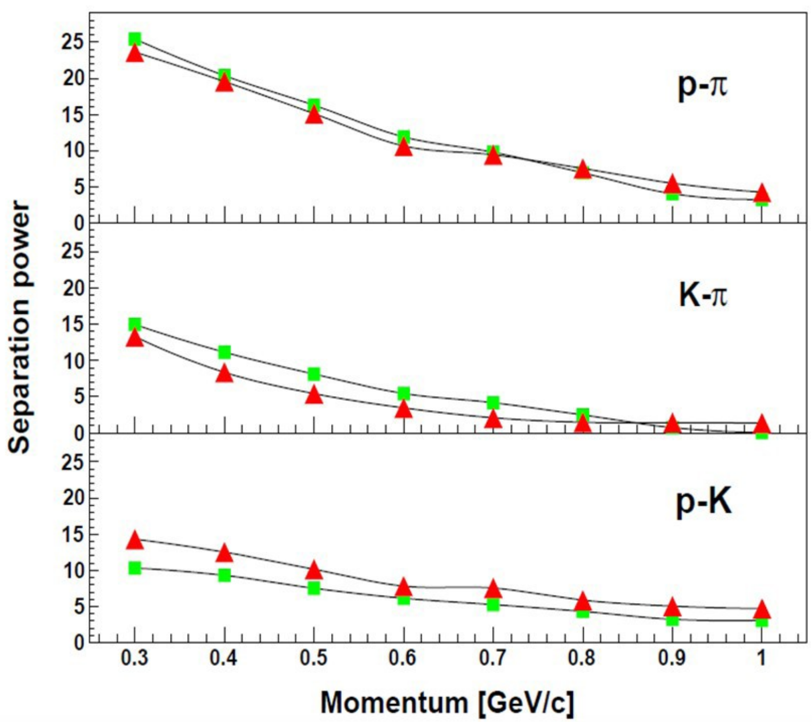


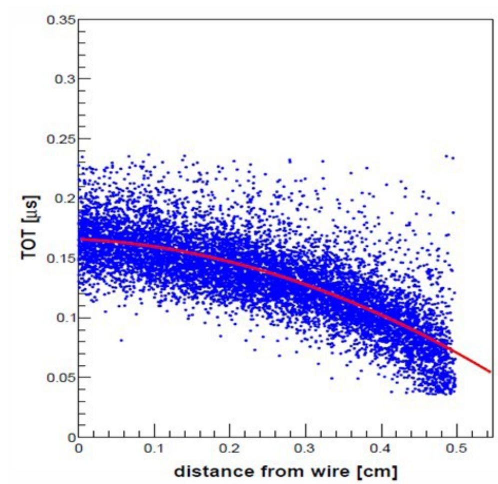


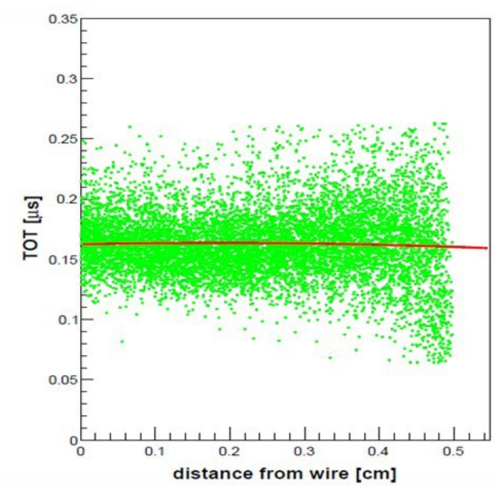


**Sedigheh Jowzaee et al.**

# Evidences of Cerenkov light from a $TeO_2$ Crystal

- measurement of Cherenkov light component in $TeO_2$ crystal to suppress $\alpha$ background
- ~60% of light depends on track angle, the rest probably also Cherenkov light scattered/reflected from crystal faces

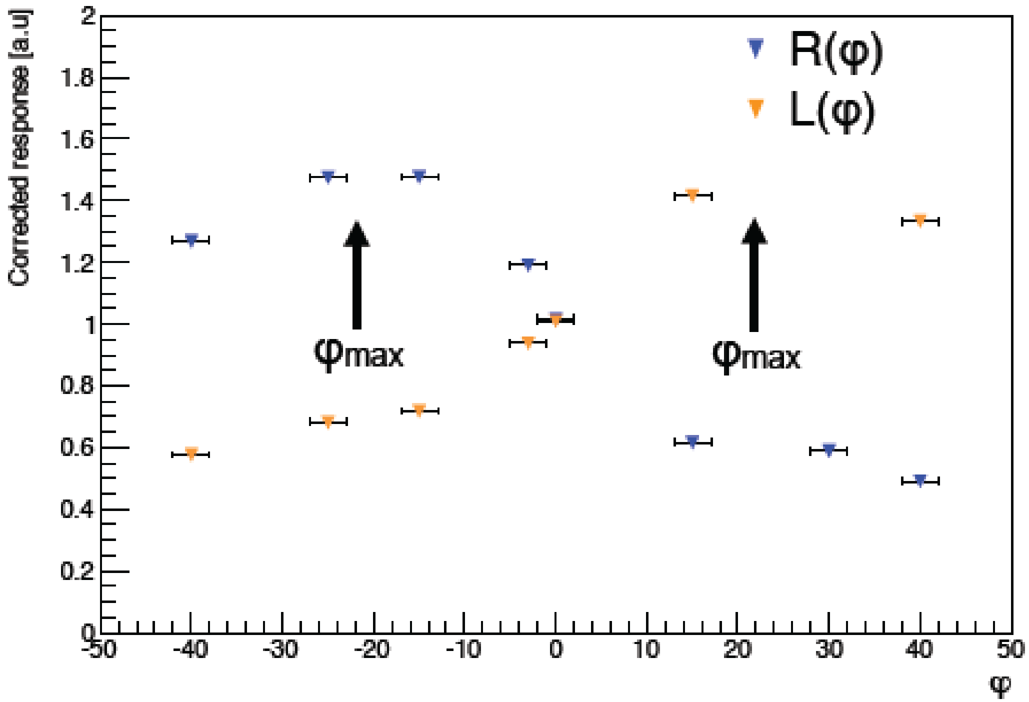


Response corrected for the muon path length and PMT gain equalize

The angle dependence is clearly visible and similar on the two sides

Experimental setup

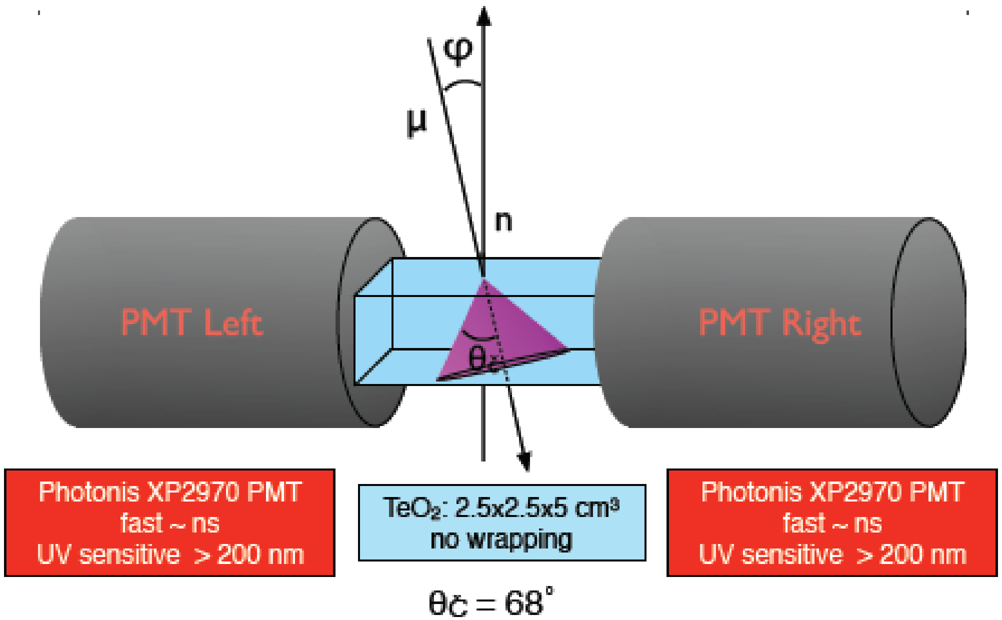


Nicola Casali et al.

# A Charged Particle Identification Detector in the Forward Region of SuperB

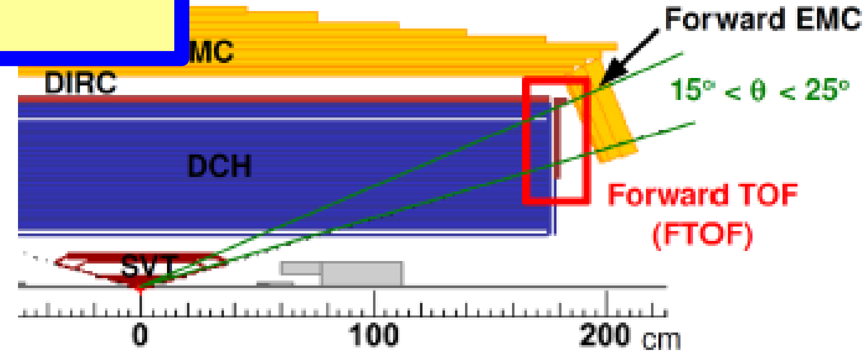


- Goal: improve PID in this angular region
  → Increase signal efficiency and/or background rejection
- Detector requirements
  - Good π/K separation up to ~3 GeV/c
  - Compact device (limited available space)
  - Small $X_0$ fraction (in front of forward calorimeter)
  - Radiation hard (close to IP)

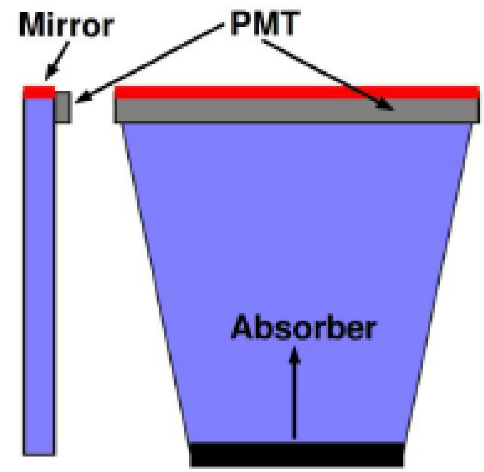


- Selected design (SLAC + LAL)
  - Thin (1.5 cm) fused silica tiles
  - Charged particles produce Cherenkov light
  - Photons trapped by total internal reflection are detected by MCP-PMTs
  - Optimization criteria: ↑ photon yield; ↓ timing spread
  - 2D-device: γ time and position (+ tracking information) used to ID particles
- ~2 meter flight length from IP
  → Total accuracy needed: ~30 ps / track
- Very fast MCP PMTs needed
  → E.g. Hamamatsu SL-10
- New ultra-fast electronics: the USB WaveCatcher (LAL + Irfu)
  - Accuracy better than 10 ps
  → See poster in front-end session

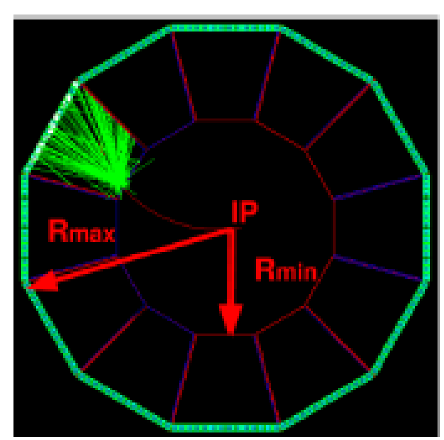


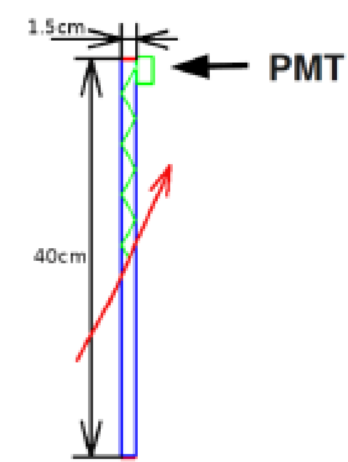


Nicolas Arnaud et al.

- Current design: 12 Fused Silica tiles
  168 MCP-PMTs
  672 channels

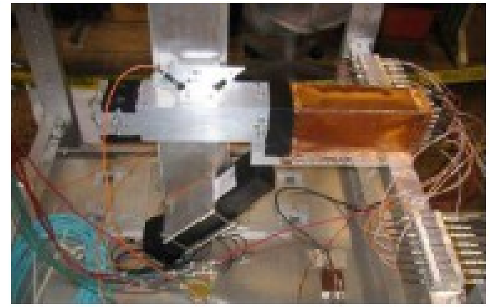

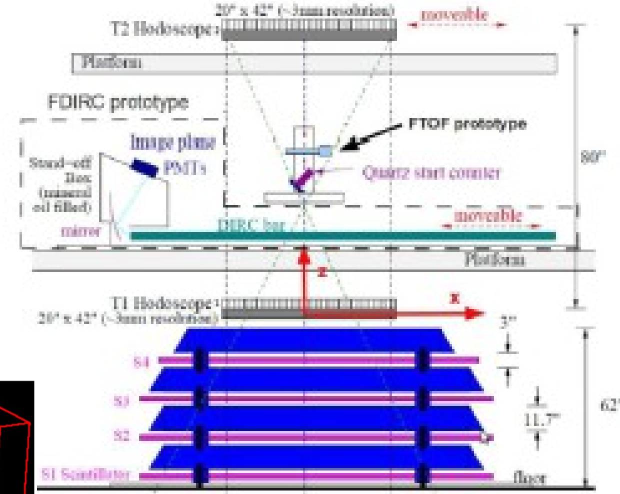


- Promising test in the SLAC Cosmic Ray Telescope
  - 16-channel electronics with 10 ps accuracy
  - Excellent data-simulation (G4) agreement
  - Waveform analysis
  - Time differences between channels
  
  → ~80 ps / photon / channel (preliminary)

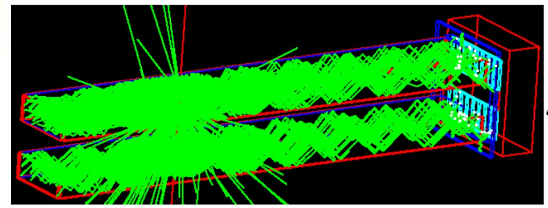

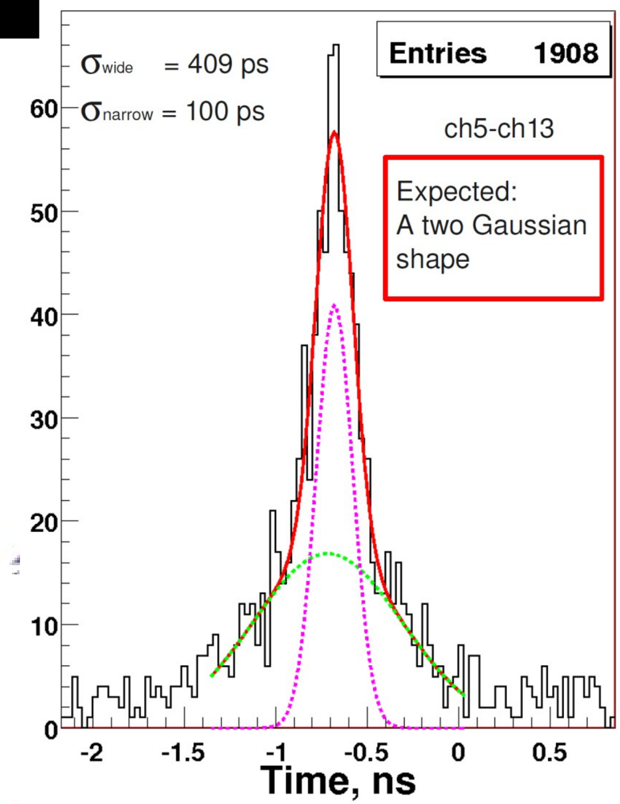


- Challenges
  - Reconstruction
  - Background (MCP-PMT integrated charge)
  - Integration in the SuperB detector

- Next steps
  - Purchase detector components (quartz, MCP-PMTs)
  - Complete electronics development
  - Build a full size sector; test it – cosmics, beam
  
  → Become part of the SuperB baseline

- Opportunties for collaborators to join
- Contact: Nicolas ARNAUD (narnaud@lal.in2p3.fr)

Laboratoire de l'Accélérateur Linéaire (IN2P3/CNRS & Université Paris Sud)

Nicolas Arnaud et al.

# Active TARget
## (Particle ID, position and timing measurement with scintillating fibers readout by SiPMs)

- The thinnest and fast available scintillating fibers coupled to SiPM
  - to detect minimum ionizing and stopping particles in high magnetic field (1.5 Tesla) environment
  - to substain high beam rate (up few x $10^8$ particles/s)
  - to provide superior position (<100 μm) and excellent timing resolutions (< 500 ps @ 10phe)

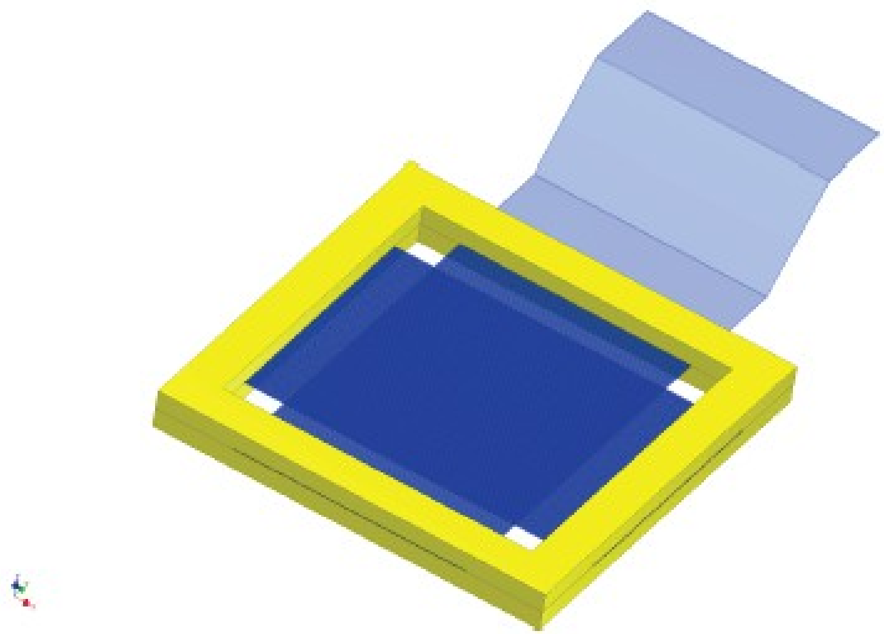

**Scintillating medium**

*Squared 250 x 250 um2 multi-clad scintillating fibers BCF12 (Saint-Gobain, peak emission @ 435 nm) with a light yield of ~8000 ph/MeV, a trapping efficiency of 7.3% , 1/e length 2.7 m and a time decay of 3.2 ns are the detection medium.*

**Photon detector**

*SiPM will be used to detect extremely weak light and to be operated in an high magnetic field (1.3 Tesla). Each Fiber is readout by a single detector. The detector efficiency is optimized using the SiPM with the higher PDE (65%) and gain(2.4 x 10^6), and low dark current rate (600 KHz@0.5phe).*

**HAMAMATSU S10362-11-100C**

Angela Papa et al.

Electronics

- It can give
  - a measurement of high beam intensity and 2-dimensional beam profile
  - coupled with a spectrometer, a measurement of decay vertex and timing with improvement of the particle momentum and angular variables resolutions
  - particle ID (muons/positrons)

- **FRONT-END**
  - smart and low-noise board (<10mV peak-to-peak)
  - amplification factor: 10
  - tunable input attenuation and output shape
- **5 GHz waveform digitizer**
  - sampling speed up to 5 GSPS
  - excellent time and amplitude performances
  - custom analysis waveform (pile-up rejection, template, after-pulse tagging etc.)

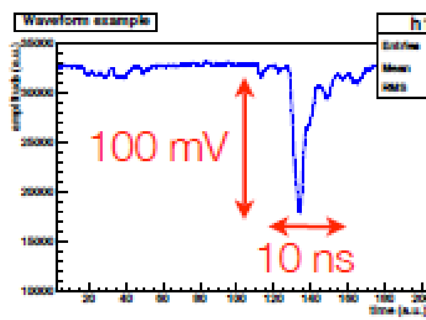


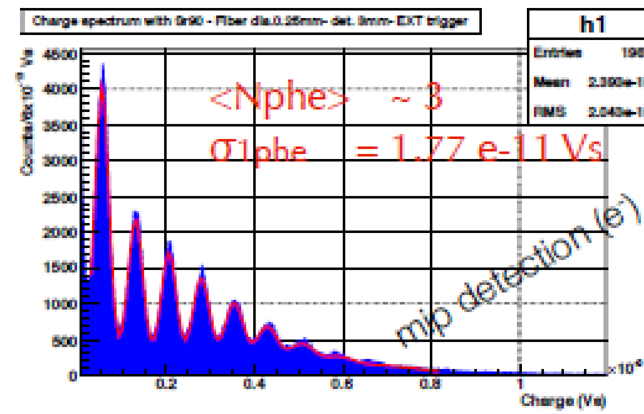


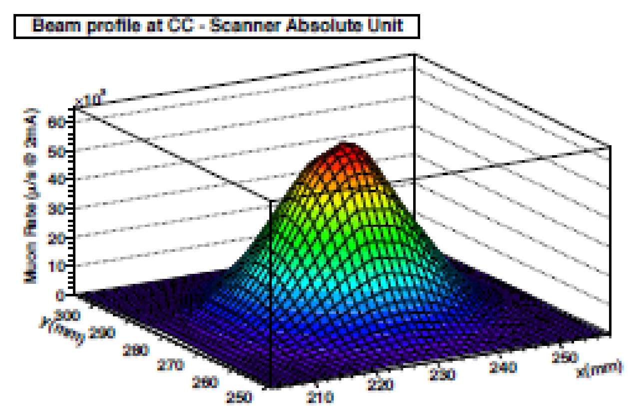


Results and prospect

**Angela Papa et al.**

# The large-angle photon veto system for the NA62 experiment at CERN

- measurement of K->πνν requires strong suppression of channels with γ's (ππ$^0$)
- development and tests of lead glass calorimeter with TOT electronics is described
- simulation and beam test results are presented and agree very well

## Lead glass blocks from OPAL

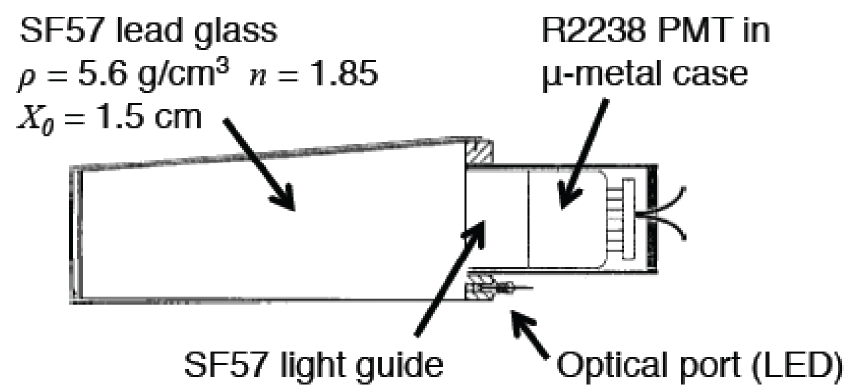


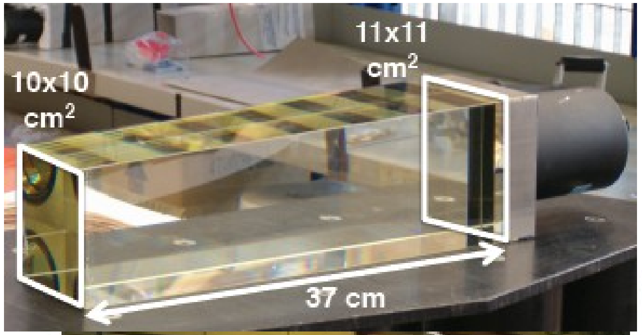



Complete LAV station at CERN, ready for installation

### Charge reconstruction

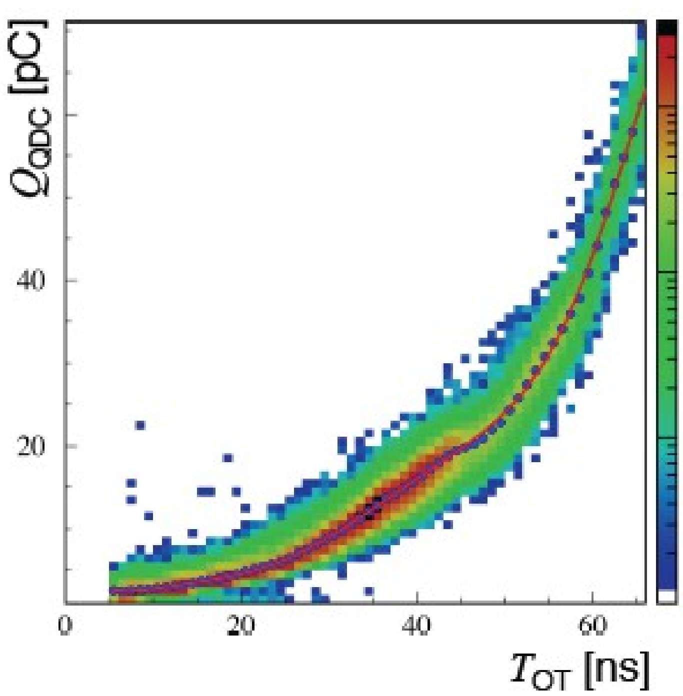


### Energy resolution

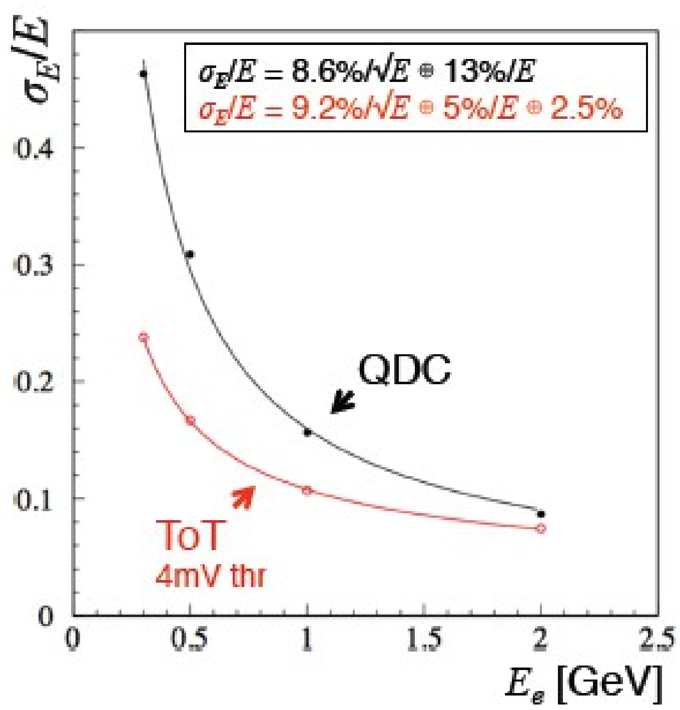



**Paolo Massarotti et al.**

# The MICE beamline instrumentation for a precise emittance measurement

• Muon Ionization Cooling Experiment (MICE) to study muon beamcooling, major step towards a "neutrino factory" and a "muon collider"

• muon purity is assured by three Time-of-Flight (TOF) measurements  (50ps), two threshold Cherenkovs (μ/π), and a low energy muon/electron ranger KL/EMR (μ/e).

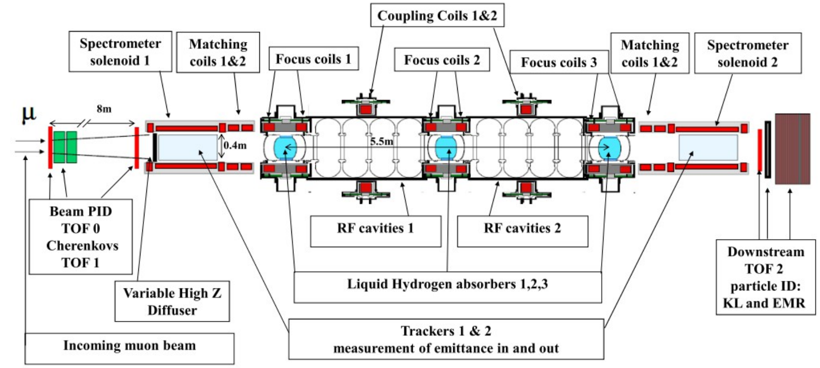


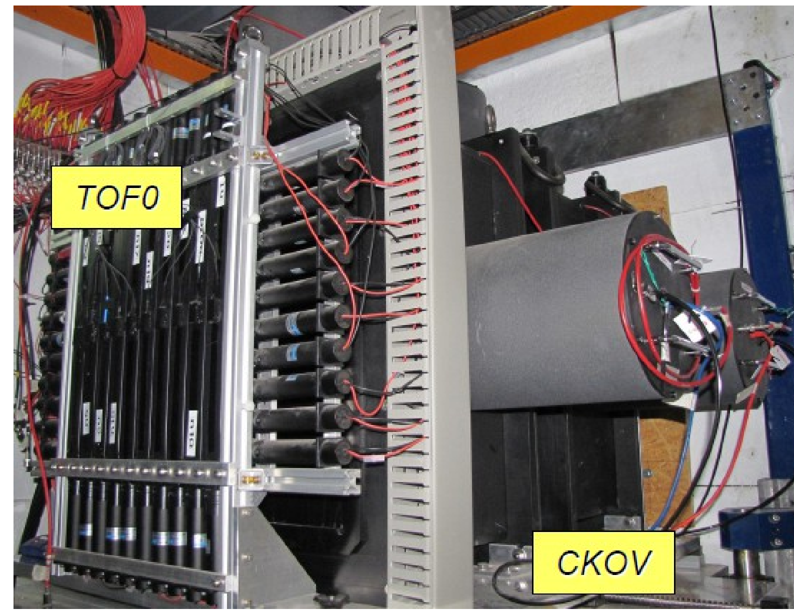


| | $P^{th}\mu$(MeV/c) | $P^{th}\pi$(MeV/c) |
|---|---|---|
| Aerogel 1.12 | 220 | 280 |
| Aerogel 1.07 | 280 | 360 |

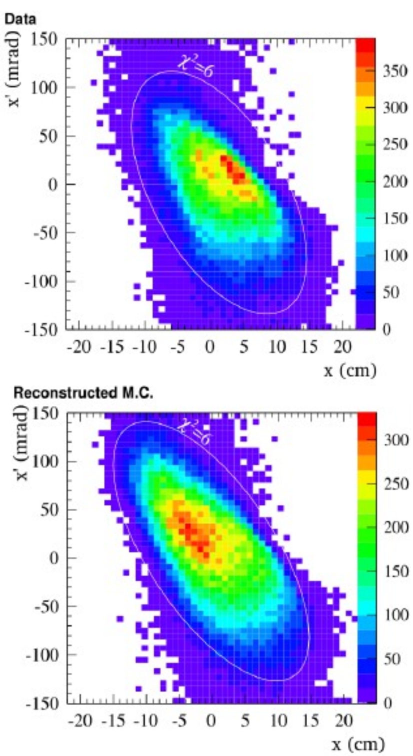


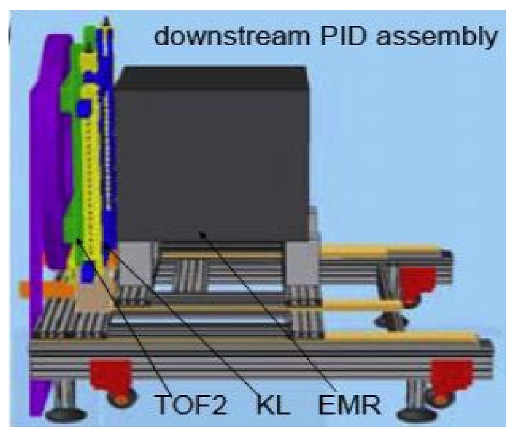


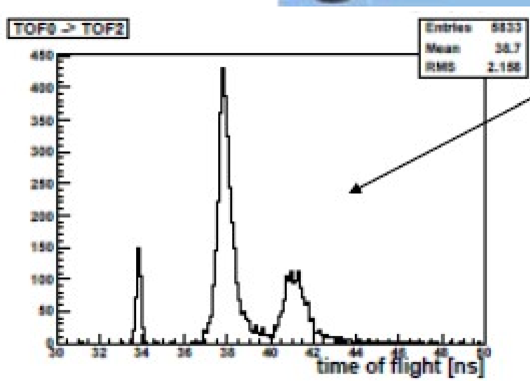


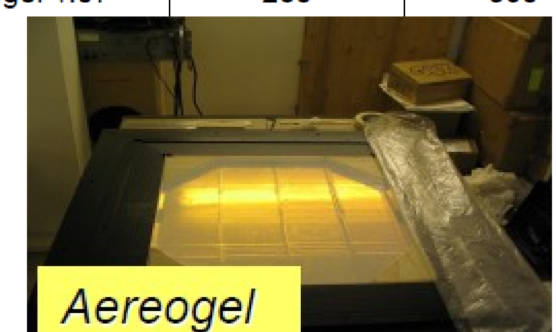


**Christopher Heidt et al.**

# KLOE-2 High Energy Tagger Detector

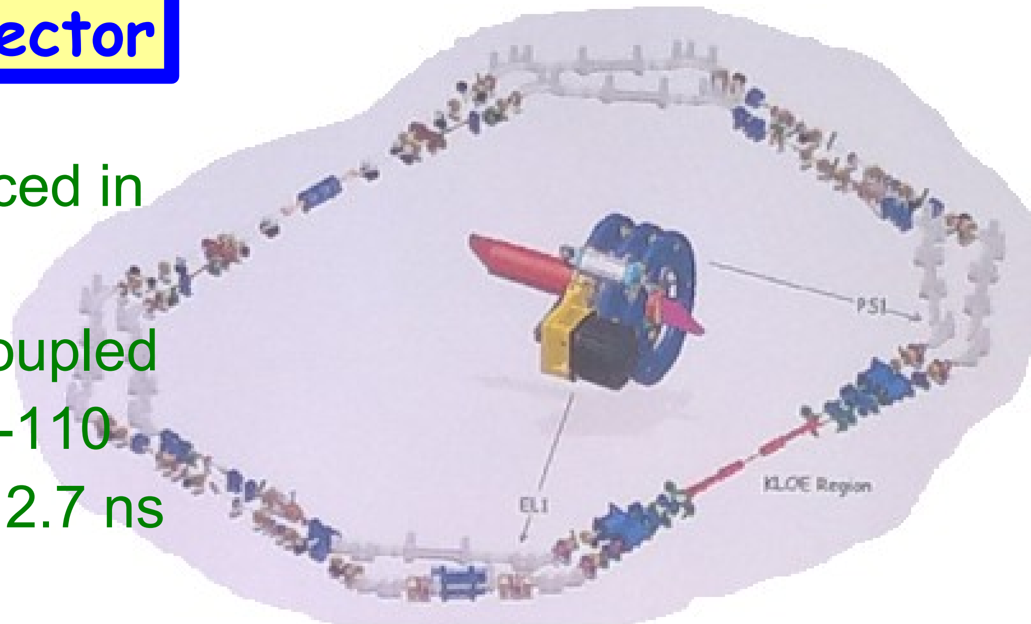


- two high energy taggers (HET) are placed in DAΦNE ring to tag γγ events
- each HET has 28 plastic scintillators coupled to HAMAMATSU high QE PMT R9880U-110
- timing resolution should be better than 2.7 ns for synchronization with KLOE-2
- detector is currently in commissioning phase and preliminary results agree with expectations

HET readout : a custom TDC multihit

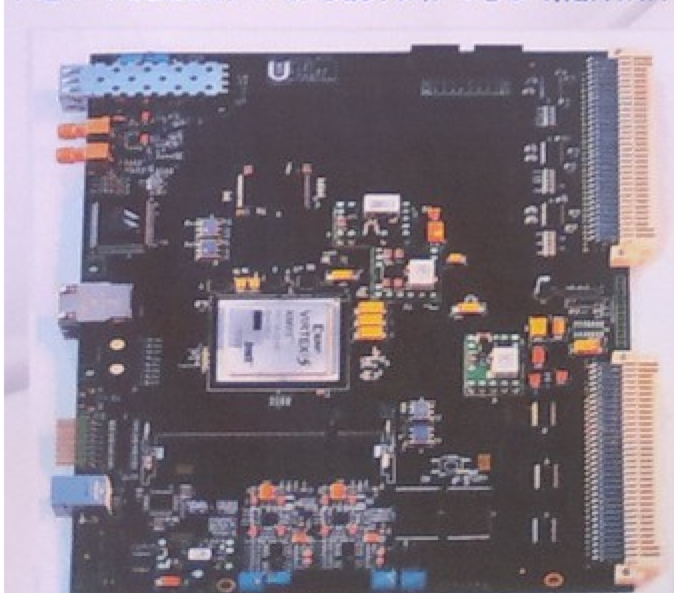

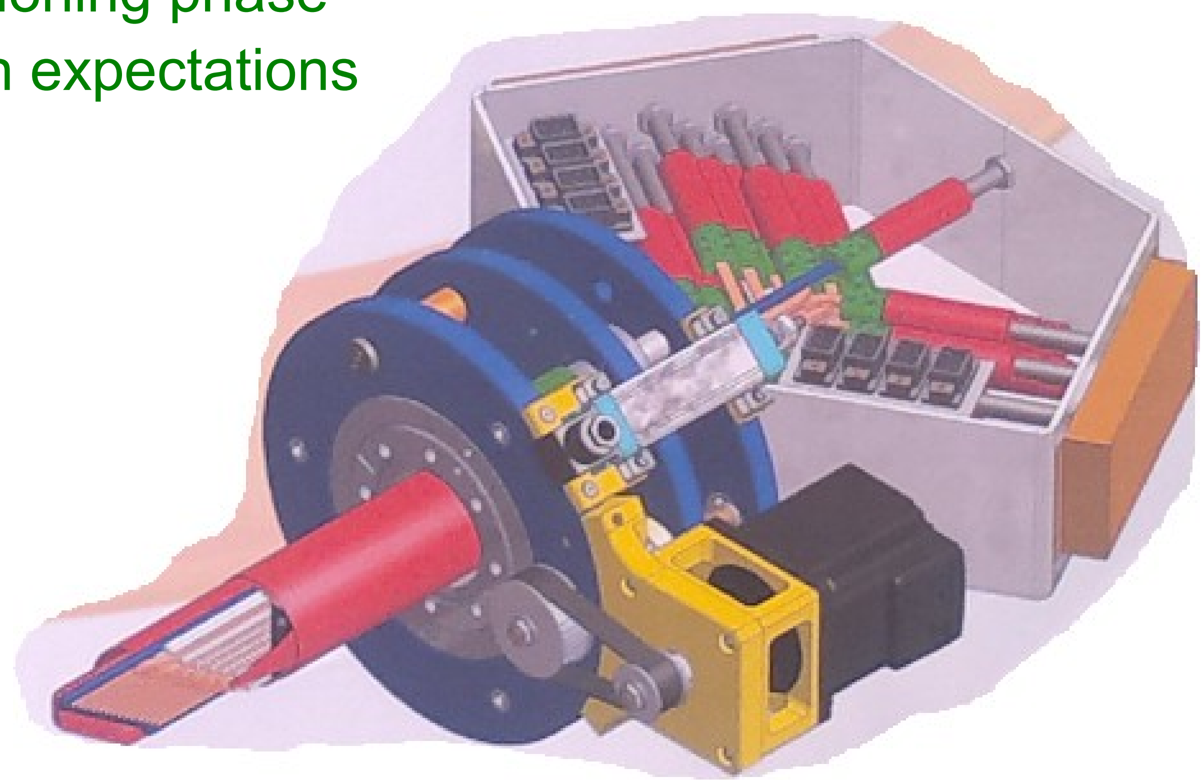

**Dario Moricciani et al.**

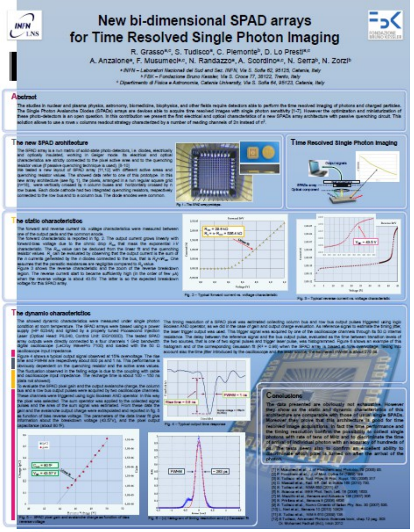
New bi-dimensional SPAD arrays
for Time Resolved Single Photon Imaging
Abstract
The new SPAD architecture
Time Resolved Single Photon Imaging
The static characteristics
The dynamic characteristics
Conclusions

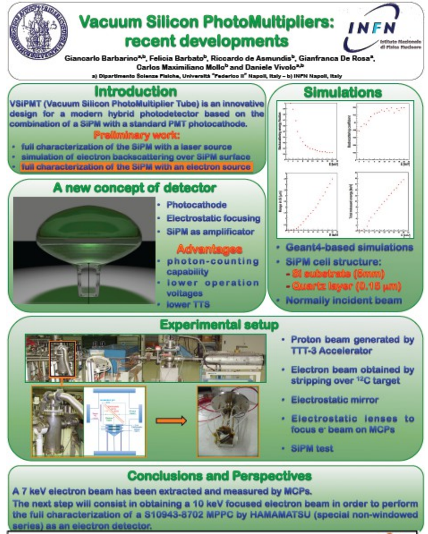
Vacuum Silicon PhotoMultipliers:
recent developments
INFN
Introduction
Simulations
Preliminary work:
A new concept of detector
Photocathode
Electrostatic focusing
SiPM as amplifier
Advantages
Geant4-based simulations
Normally incident beam
Experimental setup
Electrostatic mirror
SiPM test
Conclusions and Perspectives

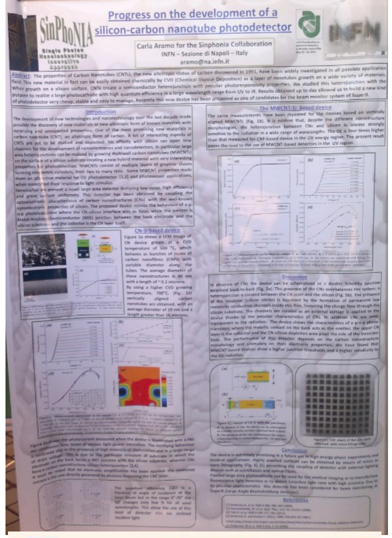
Progress on the development of a
silicon-carbon nanotube photodetector

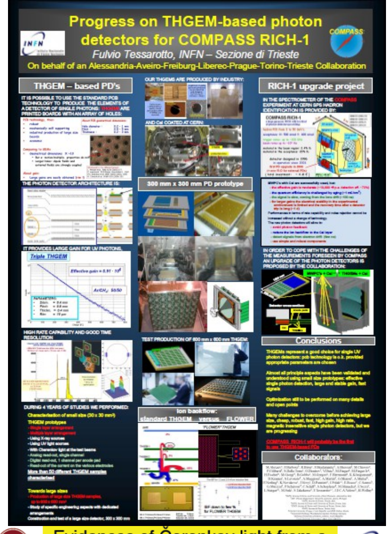
Progress on THGEM-based photon
detectors for COMPASS RICH-1
Fulvio Tessarotto, INFN – Sezione di Trieste
THGEM – based PD's
RICH-1 upgrade project
300 mm x 300 mm PD prototype
Conclusions
Collaborators:

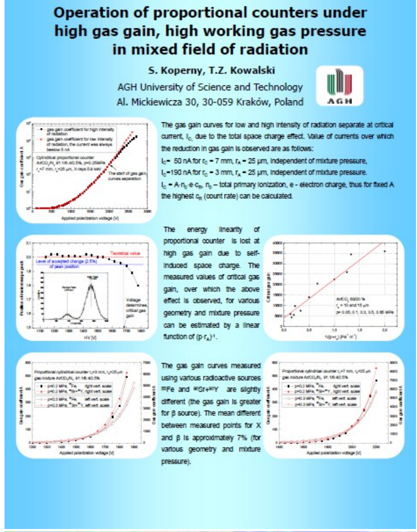
Operation of proportional counters under
high gas gain, high working gas pressure
in mixed field of radiation
S. Koperny, T.Z. Kowalski
AGH University of Science and Technology
Al. Mickiewicza 30, 30-059 Kraków, Poland
AGH

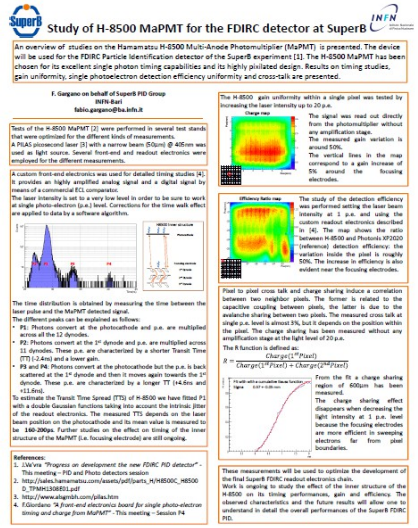
SuperB
Study of H-8500 MaPMT for the FDIRC detector at SuperB
INFN
References:

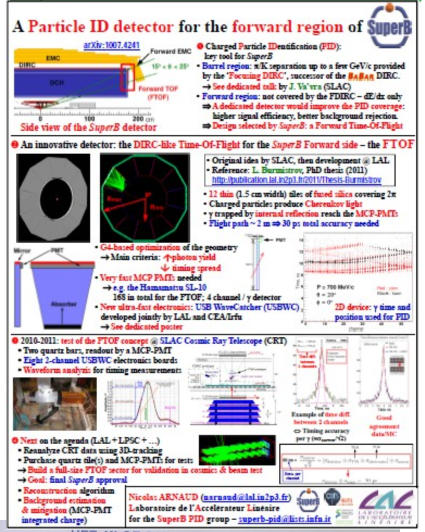
A Particle ID detector for the forward region of SuperB
Side view of the SuperB detector
An innovative detector: the DIRC-like Time-Of-Flight for the SuperB Forward side – the FTOF
Laboratoire de l'Accélérateur Linéaire

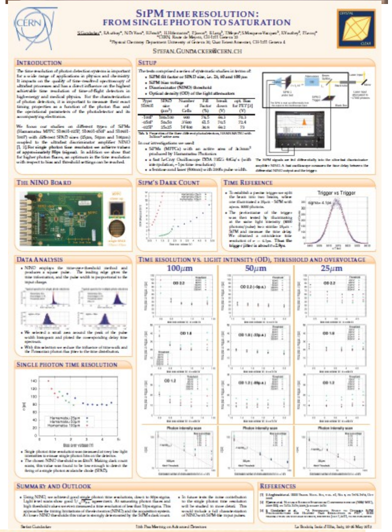
SiPM TIME RESOLUTION:
FROM SINGLE PHOTON TO SATURATION
CERN
Introduction
Setup
The NINO Board
SiPM's Dark Count
Time Reference
Data Analysis
Single Photon Time Resolution
Summary and Outlook
References

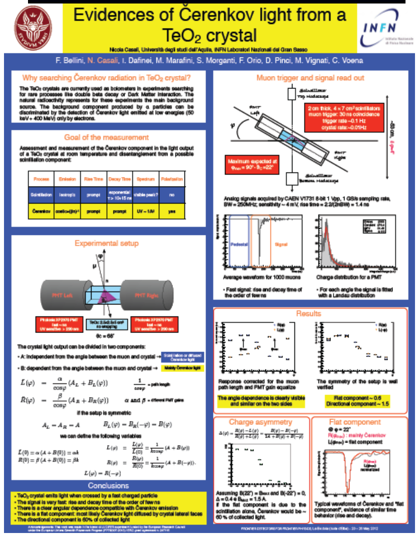
Evidences of Čerenkov light from a
$TeO_2$ crystal
INFN
Why searching Čerenkov radiation in $TeO_2$ crystal?
Muon trigger and signal read out
Goal of the measurement
Experimental setup
Results
Conclusions

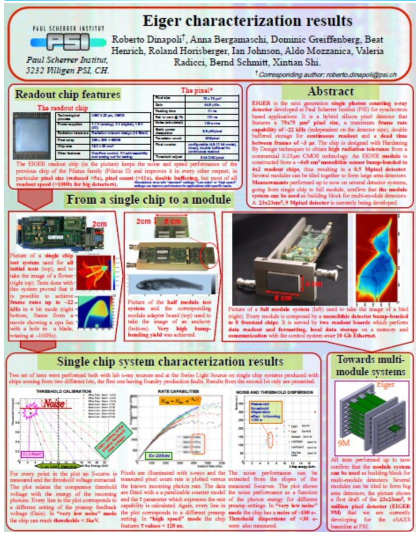
Eiger characterization results
PAUL SCHERRER INSTITUT
PSI
Readout chip features
Abstract
From a single chip to a module
Single chip system characterization results
Towards multi-module systems

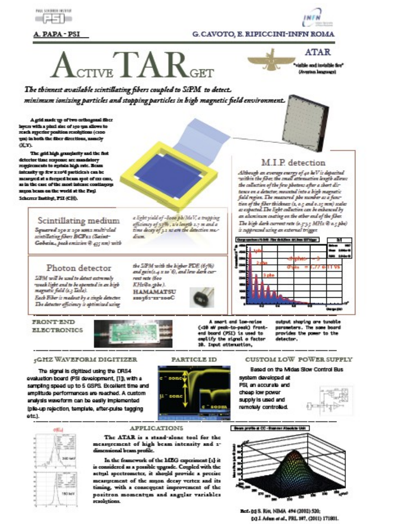
ACTIVE TARGET
ATAR
M.I.P. detection
Scintillating medium
Photon detector
FRONT-END ELECTRONICS
PARTICLE ID
CUSTOM LOW POWER SUPPLY
APPLICATIONS

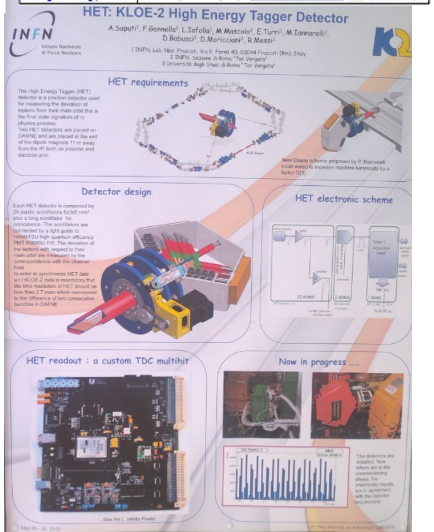
HET: KLOE-2 High Energy Tagger Detector
INFN
HET requirements
Detector design
HET electronic scheme
HET readout : a custom TDC multihit
Now in progress ...

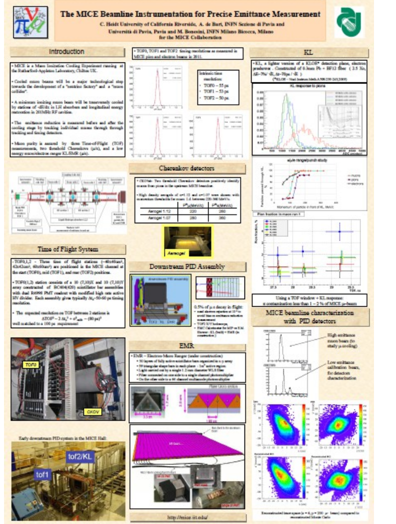
The MICE Beamline Instrumentation for Precise Emittance Measurement
Introduction
Cherenkov detectors
Time of Flight System
Downstream PID Assembly
EMR
MICE beamline characterization with PID detectors

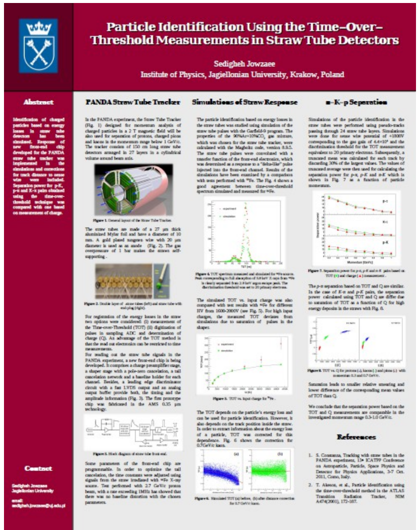
Particle Identification Using the Time-Over-
Threshold Measurements in Straw Tube Detectors
Sedigheh Jowzaee
Institute of Physics, Jagiellonian University, Krakow, Poland
Abstract
PANDA Straw Tube Tracker
Simulations of Straw Response
References
Contact

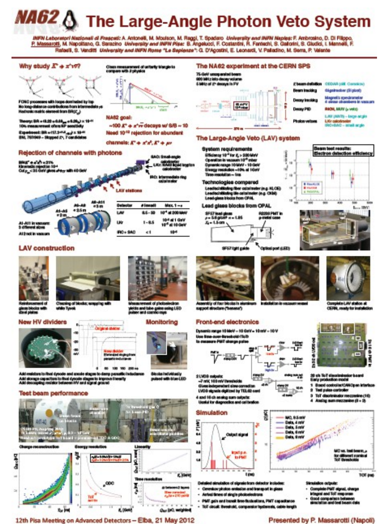
NA62
The Large-Angle Photon Veto System
The NA62 experiment at the CERN SPS
LAV construction
New HV dividers
Monitoring
Front-end electronics
Test beam performance
Simulation
12th Pisa Meeting on Advanced Detectors – Elba, 21 May 2012
Presented by P. Massarotti (Napoli)

# BACKUP SLIDES

| | | |
|---|---|---|
| 18:41 | EIGER characterization results ( Poster ; Slides ) | Roberto Dinapoli (*Paul Scherrer Institut*) |
| 18:41 | Influence of Gamma-Radiation on CdZnTe Crystals Polarization in Alternating Electric Field | Oleksii Poluboiarov (*Institute for Single Crystals*) |
| 18:41 | Vacuum Silicon PhotoMultipliers ( Poster ) | Daniele Vivolo (*INFN - Napoli*) |
| 18:41 | Progress on the Development of a Silicon-Carbon Nanotube Photodetector | Carla Aramo (*INFN - Napoli*) |
| 18:41 | Progress on THGEM-based photon detectors for COMPASS RICH-1 ( Poster ) | Fulvio Tessarotto (*TS*) |
| 18:41 | Optimisation of SiPM Intrinsic and Coincidence Time Resolution Using Digital Techniques | Paola Avella (*University of Surrey*) |
| 18:41 | New bi-dimensional SPAD arrays for Time Resolved Single Photon Imaging ( Poster ; Slides ) | Rosaria Grasso (*UNICT*) |
| 18:41 | Operation of proportional counters under high gas gain, high working gas pressure in mixed field of radiation. ( Poster ) | Stefan Koperny (*AGH, University of Science and Technology, Faculty of Physics and Applied Computer Science*) |
| 18:41 | KLOE-2 High Energy Tagger Detector | Dario Moricciani (*ROMA2*) |
| 18:41 | A Charged Particle Identification Detector in the Forward Region of SuperB ( Poster ; Slides ) | Nicolas Arnaud (*LAL-Orsay*) |
| 18:41 | The large-angle photon veto system for the NA62 experiment at CERN | Paolo Massarotti (*Naples University & INFN*) |
| 18:41 | Study of H-8500 MaPMT for the FDIRC detector at SuperB ( Poster ; Slides ) | Fabio Gargano (*INFN - Bari*) |
| 18:41 | Test Beam Results of the SuperB Muon Detector Prototype | Gianluigi Cibinetto (*INFN Ferrara*) |
| 18:41 | Particle ID, position and timing measurement with scintillating fibers readout by SiPMs ( Poster ; Slides ) | Angela Papa (*Paul Scherrer Institut*) |
| 18:41 | Photodetector time resolution : from single photons to saturation ( Poster ) | Stefan Gundacker (*CERN*) |
| 18:41 | The MICE beamline instrumentation for a precise emittance measurement | Christopher Heidt (*University of California Riverside*) |
| 18:41 | Particle identification using the time-over-threshold measurements in straw tube detectors ( Poster ) | Sedigheh Jowzaee (*Institute of Physics, Jagiellonian University, Krakow, Poland*) |
| 18:41 | Evidences of Cerenkov light from a TeO$_2$ Crystal ( Poster ) | Nicola Casali (*INFN Laboratori Nazionali del Gran Sasso*) |

# A Charged Particle Identification Detector in the Forward Region of SuperB

Nicolas Arnaud et al.

# New bi-dimensional SPAD arrays for Time Resolved Single Photon Imaging

## What is time resolved single photon imaging

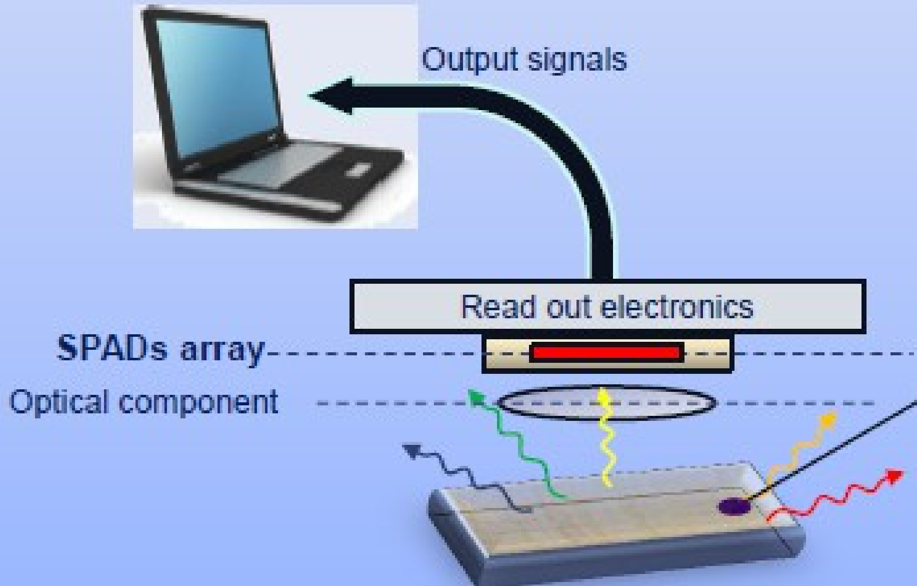


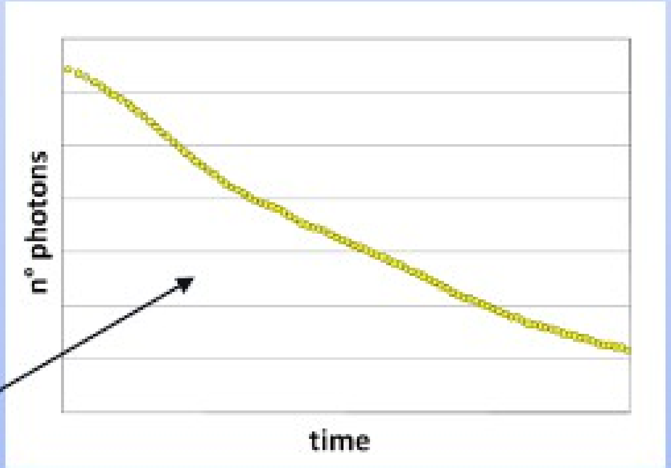


Time trend decay of photons emitted by unit area and acquired by one pixel of SPADs array

## The new SPAD array architecture

The diodes are arranged in a n×n regular square grid (n=18), vertically crossed by n column buses and horizontally crossed by n row buses. Each diode cathode have two integrated quenching resistors, respectively connected to the row bus and to a column bus. The diode anodes are common.

Example of juction scheme of SPAD device

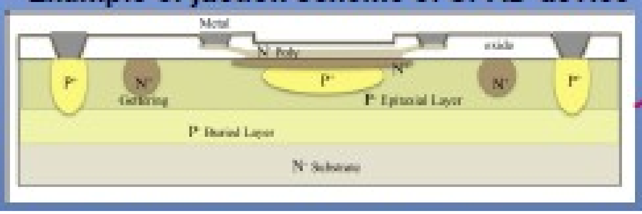

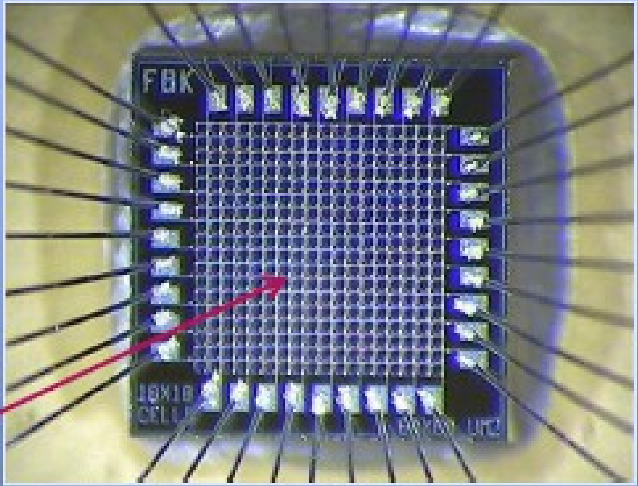

Prototype of SPAD array

Rosaria Grasso et al.

## Static characteristics

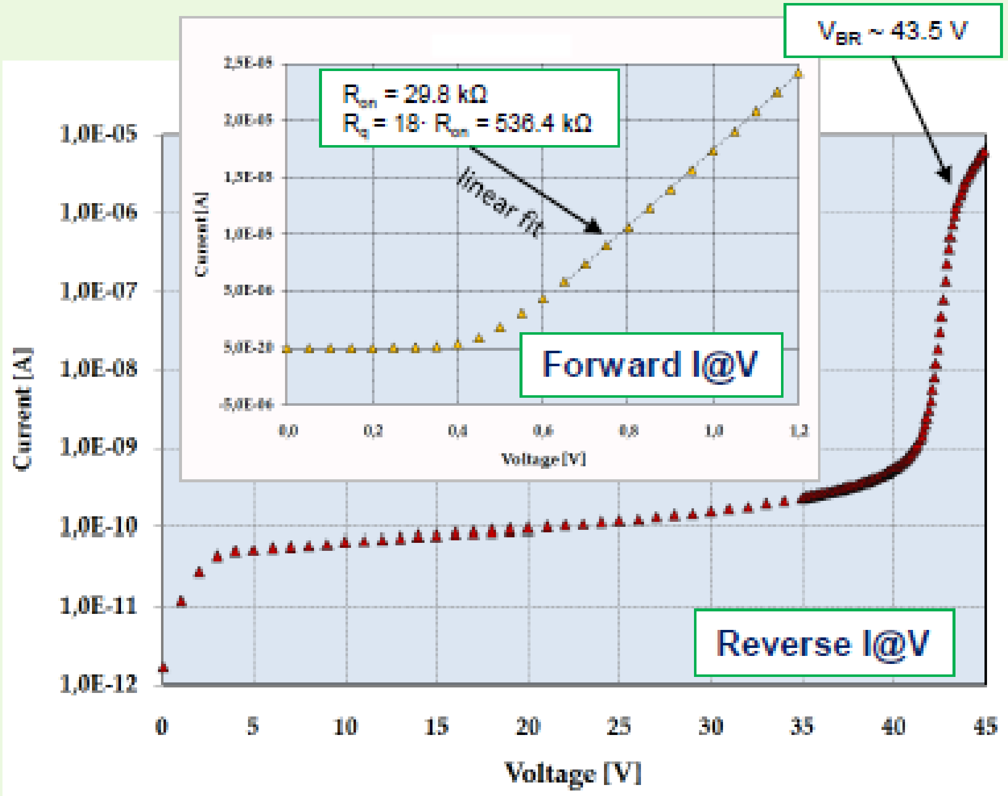


## Output time response

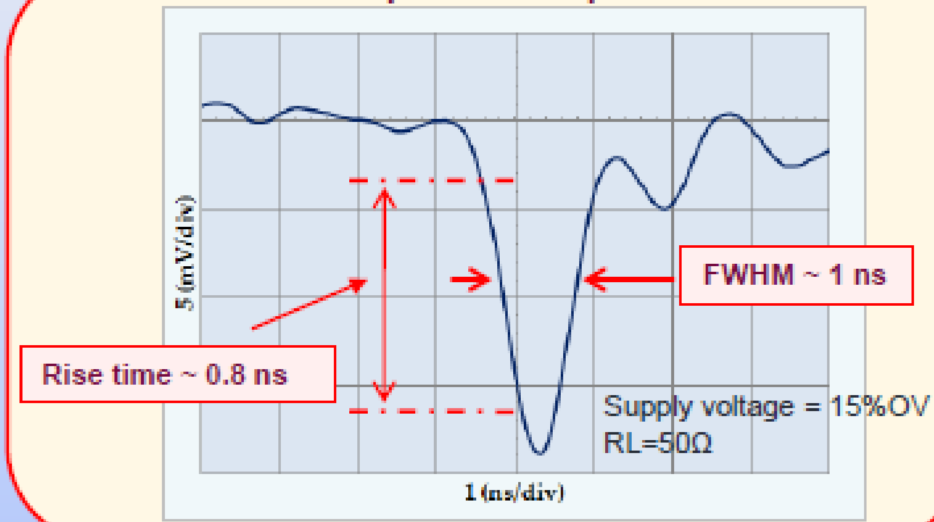


## Gain and avalanche charge Vs. bias reverse voltage

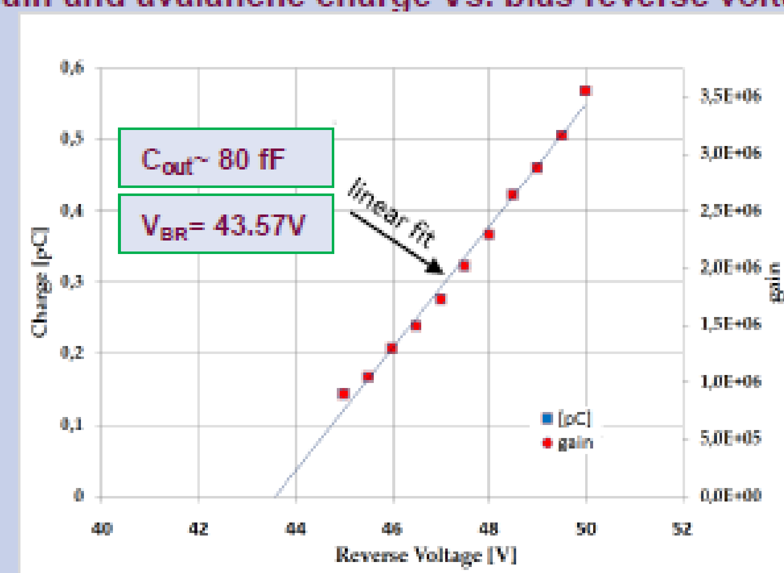


## Timing resolution

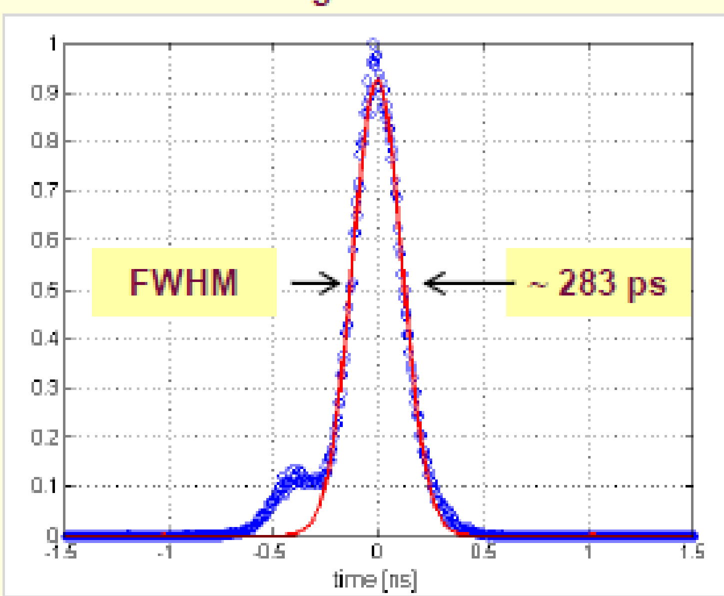


*S. Tudisco et al.*, NIM A 610 (2009) 138.

*S.Tudisco*, Advanced Photonic Sciences book, chap.12 pag. 303

Dr. Mohamed Fadhali (Ed

**Rosaria Grasso et al.**

# EIGER characterization results

Roberto Dinapoli†, A. Bergamaschi, D. Greiffenberg, B.Henrich, R. Horisberger, I. Johnson, A. Mozzanica, V. Radicci, B. Schmitt, X. Shi

## Main features

| | |
|---|---|
| Detector type | Hybrid (silicon), single photon counting, pixel |
| Pixel size | 75 x 75 $\mu m^2$ |
| Chip size | 19.3 x 20 $mm^2$ |
| Pixel array | 256 x 256 = 65536 |
| Technol. process | UMC 0.25 μm |
| Radiation tolerance | Rad hard design (>4Mrad) |
| Pixel counter | 12 bits, binary, double buffered for continuous readout, configurable (4,8,12 bit mode) |
| Threshold adjust. | 6 bit DAC/pixel |
| Frame rate | Up to 23 kHz, indep. on the detector size |

## Characterization results

| | |
|---|---|
| Minimum noise (very low noise mode) | <100 e- |
| Threshold dispersion | <30e- (trimmed) |
| Rate capability (high speed mode) | $\tau$ < 130 ns |
| Minimum threshold (very low noise mode) | <3 keV |
| Measured frame rate (4 bit mode) | Up to 22 kHz |

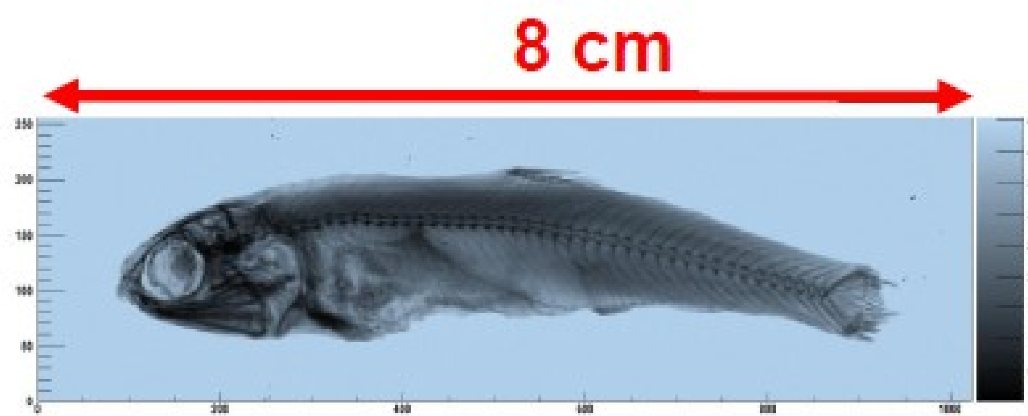

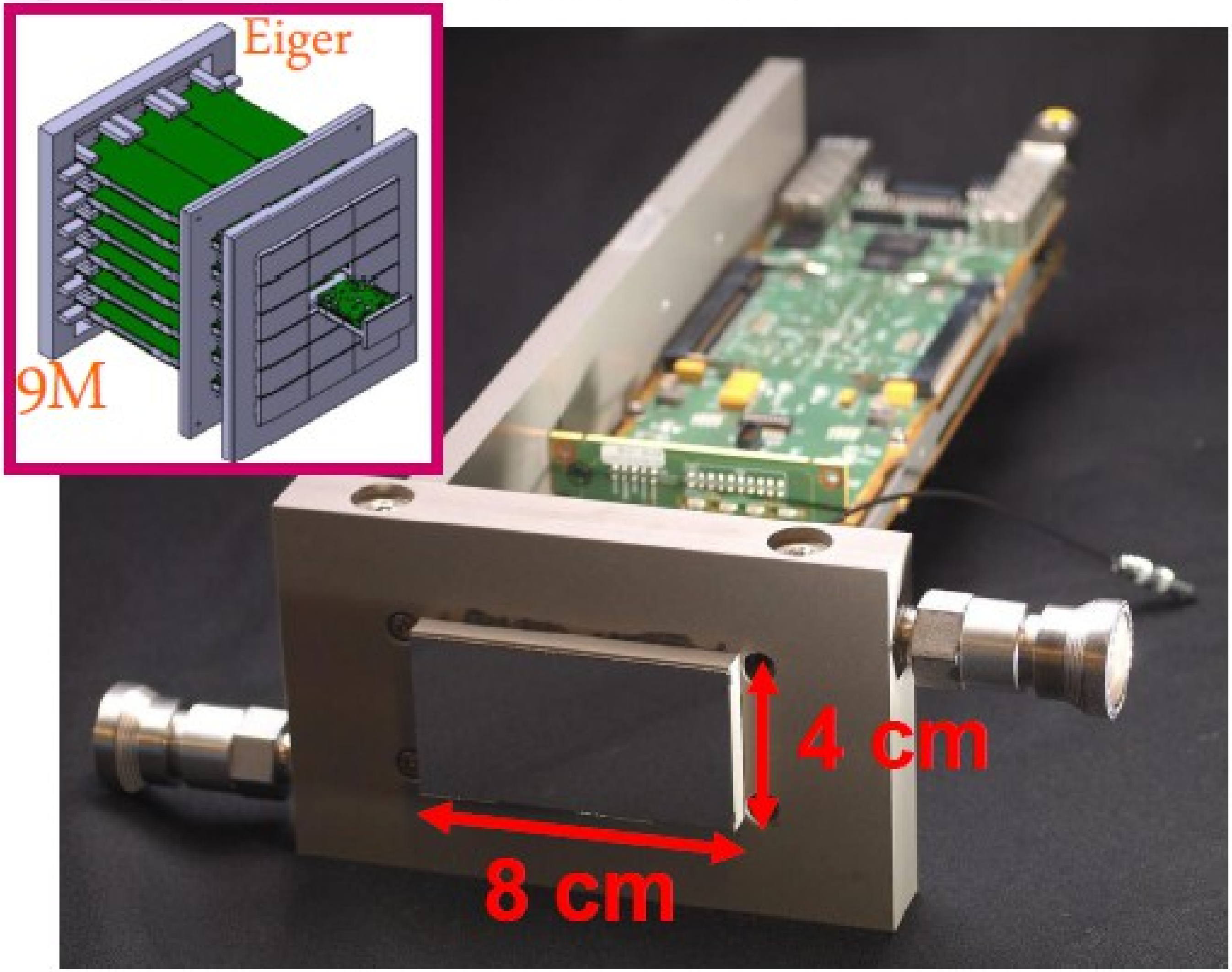


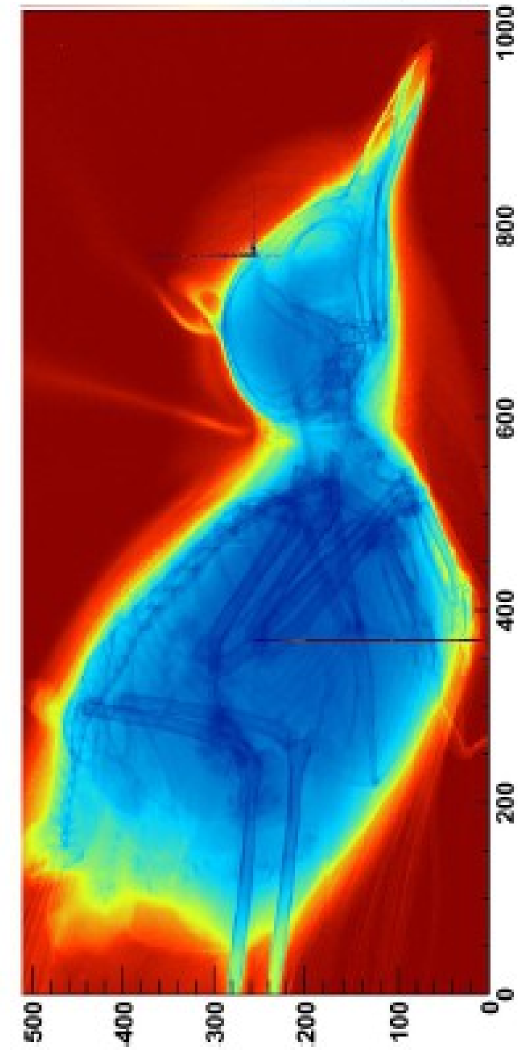


Picture of a **full module system** (left) used to take the image of a bird (right). Every module is composed by a **monolithic detector bump-bonded to 8 frontend chips**. It is served by **two readout boards** which perform **data readout and formatting, local data storage** on a memory and **communication** with the control system **over 10 Gb Ethernet.** Several modules can be tiled together to form large area detectors. A **23x23cm², 9 Mpixel, 22 kHz maximum frame rate detector** (**EIGER 9M,** shown in the top left corner) is currently being developed.